Electronic Supplementary Information

Constrained beta-amino acid-containing miniproteins

Magda Drewniak-Świtalska[a], Barbara Barycza[a], Ewa Rudzińska-Szostak[a], Paweł Morawiak[a], Łukasz Berlicki[a]*

[a]*Department of Bioorganic Chemistry, Wrocław University of Science and Technology, Wybrzeże Wyspiańskiego 27, 50-370 Wrocław, Poland,*

E-mail: lukasz.berlicki@pwr.edu.pl.

Table of contents

Peptide synthesis. All commercially available reagents and solvents were purchased from Sigma-Aldrich, Merck, Iris Biotech or Lipopharm and used without further purification. Fmoc (1*S*,2*S*)-*trans*-2-aminocyclopentanecarboxylic acid was purchased from the Synnovator and has >95% of purity. Peptide foldamers were obtained with an automated solid-phase peptide synthesizer (Biotage® Initiator+Alastra™) on H-Rink amide ChemMatrix® resin (loading: 0.59 mmol/g) in 100 mg scale. Fmoc deprotection was achieved using 20% piperidine in DMF for 3 + 10 min. A double-coupling procedure was performed with 0.5 M solution of DIC and 0.5 M solution of OXYMA in DMF, for α-amino acids 2 x 15 min, for β-amino acids 30 min, at 75 °C. Acetylation reaction was carried out using NMP/DIPEA/acetic anhydride (80:15:5) mixture. Cleavage of the peptides from the resin was accomplished with the mixture of TFA/TIS/H_2O (95:2.5:2.5) after 3 h of shaking or TFA/TIS/thioanisole/H_2O (85:5:5:5) after 4 h of shaking if in sequence was arginine residue. The crude peptide was precipitated with ice-cold diethyl ether and centrifuged (9000 rpm, 2 x 15 min, 4 °C). Obtained peptide foldamers were purified using the HPLC (Knauer Prep) with a preparative column 250 mm x 30 mm, Thermo Scientific™ Hypersil GOLD™ (C18, 12μm) and an analytical column 150 mm x 4.6 mm, Kinetex 100A (C18, 5μm). Solvents and gradients are given in Table S1. Yield of peptide synthesis was in 5-25% range. All peptides were at least 95% pure according to analytical HPLC.

Mass spectrometry. Peptides were studied by WATERS LCT Premier XE System consisting of high resolution mass spectrometer with electrospray ion source and a time of flight (TOF) analyzer (Table S2).

Circular dichroism. CD spectra were recorded on JASCO J-1500 with parameters: 0.2 nm resolution, 1.0 nm band width, 200 mdeg sensitivity, 4 s response time, 50 nm/min scanning speed. The CD spectra of the solvents alone were recorded and subtracted from the raw data. The CD intensity is given as mean residue molar ellipticity (θ [deg x cm^2 x $dmol^{-1}$]). Single CD spectra were measured at 20 °C. Peptides **1-15** were dissolved in water to 1 mg/mL concentration and diluted to 0.25 mg/mL with 100 mM potassium phosphate buffer pH 7.0. Peptides **16-29** were dissolved in 50 mM potassium phosphate buffer pH 7.0 at concentration of 1 mg/mL. Measurements were done in 0.02 cm cuvette path length and with 10 scans.

Measurement of T_m values. Solutions containing 0.25-1.00 mg/mL peptide in 100 mM potassium phosphate buffer pH 7.0 were used. Ellipticity was recorded at 222 nm using 1 mm

optical path length cuvette. The temperature was increased from 4 to 96 ^{o}C in increments of 2 ^{o}C. The melting point (T_m), was determined assuming:

$$Q_{obs} = \alpha Q_f + (1 - \alpha) Q_u$$

where: Q_{obs} – observed ellipticity, Q_f – ellipticity of folded miniprotein, Q_u – ellipticity of unfolded miniprotein, α – degree of folding;

Folded and unfolded ellipticities are linear function of temperature (T):

$$Q_f = m_f T + b_f$$

$$Q_u = m_u T + b_u$$

Where: m_f, b_f, m_u and b_u are coefficients of linear dependences.

Subsequently:

$$\alpha = \frac{1}{1 + K}$$

$$K = e^{-\frac{\Delta G^0}{RT}}$$

where: K – equilibrium constant, ΔG^0 - Gibbs free energy, R – gas constant.

Assuming heat capacity equal zero for mini-protein, Gibbs free energy can be evaluated as [S1]:

$$\Delta G^0 = \Delta H_m \left(1 - \frac{T}{T_m}\right)$$

where: ΔH_m – enthalpy; T_m – melting point temperature.

Combining all above equations, the dependence of observed ellipticity (Q_{obs}) on temperature could be obtained:

$$Q_{obs} = \frac{1}{1 + e^{\frac{-\Delta H_m \cdot \left(1 - \frac{T}{T_m}\right)}{RT}}} \cdot \left(b_f + m_f \cdot T - b_u - m_u \cdot T\right) + b_u + m_u \cdot T$$

This equation was used in non-linear fitting algorithm of the OriginPro9 program, to fit to experimental data and obtain T_m value. In most cases m_u value was assumed to be zero.

Temperature and guanidine-dependent denaturation. To examine the thermal unfolding of the peptide, stock solutions were prepared containing 0.25 mg/mL peptide in 100 mM potassium phosphate buffer pH 7.0, with 11 different concentrations of GuHCl. Each sample was incubated at room temperature for 1.5h. Ellipticity measurements were recorded at 222 nm with 1 mm path length cuvette and 3 independent scans. Others parameters were unchanged. The temperature was increased from 4 to 96 ^oC in increments of 2 ^oC.

The results for measurements with guanidine hydrochloride were analyzed using MatLab R2016a (The MathWorks, Inc.) and assuming following dependences [S2]. The observed ellipticity (Q_{obs}) depends in the equilibrium constant K and the ellipticity of folded (Q_f) and unfolded (Q_u) states.

$$Q_{obs} = \frac{1}{1+K}(Q_u \cdot K + Q_f)$$

Parameters Q_f and Q_u depend on temperature and concentration of denaturing agent ([GuHCl]):

$$Q_u = a + bT + c[GuHCl]$$

$$Q_f = d + eT + f[GuHCl]$$

Where: a, b, c, d, e and f are coefficients in these linear dependences.

The equilibrium constant K is associated with the Gibbs free energy of peptide unfolding process (ΔG^0):

$$K = e^{\frac{-\Delta G^0}{RT}}$$

However, the value of ΔG^0 is determined by the equation:

$$\Delta G^0 = \Delta H^0 - T\Delta S^0 + \Delta C_p\left(T - T_0 + Tln\left(\frac{T_0}{T}\right)\right) - m[GuHCl]$$

Nuclear magnetic resonance. The NMR experiments were performed on Bruker Avance III 600 MHz spectrometer using a 5 mm inverse detection QCI cryoprobe. The NMR spectra of 1mg of peptide **13** dissolved in 450 μL of 50 mM phosphate buffer and 50 μM D_2O of pH 7

were recorded at temperature 285 K. The temperature was controlled to ± 0.1 K. TOCSY and NOESY experiments were performed for chemical shift and structure assignment. All NMR spectra were acquired with suppression of solvent OH signal using the excitation sculpting pulse. Typical TOCSY - homonuclear Hartman (Hahn transfer using mlev17 sequence for mixing using two power levels for excitation and spinlock) and 2D NOESY were recorded in phase sensitive mode with the spectral width of 6009 Hz in both dimensions using 2048 data points and relaxation delay of 1.5s. These spectra were acquired with 1024 increments of 22 scans for TOCSY and 104 scans for 2D NOESY. Mixing times were set at 100 ms and 200 ms for TOCSY and 2D NOESY experiments, respectively. The data were acquired and processed using Topspin 3.1 (BrukerBioSpin, Rheinstetten, Germany). The processed spectra were assigned with the help of the SPARKYprogram (Goddard, T.D.; Kneller, D.G. *Sparky*, 3rd ed.;University of California; San Francisco, CA, USA 2001).

NMR structure calculation. All chemical shifts assigned to **13** can be seen in Table S3. Intensities of NOE signals were normalized to the distance between tryptophan's *beta* hydrogens and classified as follows: 1.8 – 2.5 Å: strong, 2.5 – 3.5 Å: medium, 3.5 – 4.5: weak (Table S4). Restraints to ambiguous CH_2 protons of trans-ACPC residues were omitted, while protons attached to the same carbon atoms were assumed to be a pseudo-atom. Structures were modelled using XPLOR-NIH software and images prepared in Discovery Studio Visualizer. Initially, 50 random conformations of a peptide were generated. Restraints derived from NOE contacts with upper distance limits: strong 2.5 Å (s), medium 3.5 Å (m) and weak 5 Å (w), and the lower distance limit set to 1.8 Å, were applied. Standard protocol for NMR structure calculations implemented in Xplor-NIH was used with the following steps: a) high temperature dynamics (3500 K, 800 ps or 8000 steps), b) simulated annealing performed from 3500 K to 25 K with 12.5 K step, at each temperature short dynamics was done (100 steps or 0.2 ps); c) gradient minimization of final structure. Finally, top lower energy structures were superimposed. Structure was deposited in RCSB Protein Data Bank.

Table S1. HPLC data for studied peptides

.

No.	Analytical HPLC		Preparative HPLC	
	Retention time [min]	gradient	Retention time [min]	Gradient
1	10.086	1	30.71	4
2	11.004	1	34.85	4
3	9.797	1	28.57	4
4	10.577	1	31.72	4
5	9.667	1	28.56	4
6	10.330	1	32.29	4
7	9.728	1	28.41	4
8	9.110	1	26.80	4
9	11.479	1	35.73	4
10	8.260	2	22.73	5
11	8.400	2	31.61	4
12	8.180	2	27.70	5
13	9.020	2	41.03	5
14	10.067	2	33.92	6
15	11.744	1	31.83	5
16	7.180	3	22.22	7
17	7.340	3	23.25	7
18	7.100	3	22.53	7
19	7.347	3	24.17	7
20	7.207	3	23.24	7
21	6.980	3	22.08	7
22	7.173	3	21.60	7
23	7.400	3	22.31	7
24	7.693	3	22.78	7
25	7.273	3	22.08.	7
26	7.420	3	22.87	7
27	7.475		23.27	7
28	7.460	3	23.26	7
29	7.547	3	23.80	7

Analytical HPLC. Solvent A: 99.95% H_2O, 0.05% TFA. Solvent B: 99.95% CH_3CN, 0.05% TFA.

(1) 1: Total flow: 0.9 mL/min, t = 0 min – 90% A, t = 2 min – 90% A, t = 20 min – 10% A, t = 23 min – 10% A, t = 26 min – 90 % A.

(2) Total flow: 1 mL/min, t = 0 min – 90% A, t = 2 min – 90% A, t = 11 min – 10% A, t = 12 min – 10% A, t = 15 min – 90 % A.

(3) Total flow: 1 mL/min, t = 0 min – 90% A, t = 2 min – 90% A, t = 10 min – 10% A, t = 15 min – 10% A, t = 20 min – 90 % A.

Preparative HPLC. Solvent A: 99.95% H_2O, 0.05% TFA. Solvent B: 99.95% CH_3CN, 0.05% TFA

(4): Total flow: 10 mL/min, t = 0 min – 90% A, t = 6 min – 90% A, t = 14 min – 80% A, t = 20 min – 70% A, t = 38 – 50% A, t = 40 min – 50% A, t = 48 min – 10% A, t = 50 min – 10% A, t = 56 min – 90% A, t = 60 – 90% A.

(5): Total flow: 10 mL/min, t = 0 min – 90% A, t = 6 min – 90% A, t = 12 min – 70% A, t = 20 min – 70% A, t = 38 – 60% A, t = 40 min – 60% A, t = 48 min – 10% A, t = 50 min – 10% A, t = 60 min – 90% A.

(6): Total flow: 10 mL/min, t = 0 min – 90% A, t = 6 min – 90% A, t = 12 min – 70% A, t = 20 min – 60% A, t = 68 – 20% A, t = 70 min – 20% A, t = 78 min – 10% A, t = 80 min – 10% A, t = 90 min – 90% A.

(7)Total flow: 10 mL/min, t = 0 min – 90% A, t = 6 min – 90% A, t = 23 min – 50% A, t = 25 min – 10% A, t = 30 – 10% A, t = 33 min – 90% A.

Table S2. Description of MS spectra of peptides **1**-**29**

peptide	MS found [m/z]	MS theoretical [m/z]	Difference for major peak [ppm]
1	1106.0737 ([M+2H]$^{2+}$), 737.7387 ([M+3H]$^{3+}$),	1106.0732 ([M+2H]$^{2+}$), 737.7181 ([M+3H]$^{3+}$),	0.5
2	1104.5883 ([M+2H]$^{2+}$), 744.0534 ([M+2H+Na/K]$^{3+}$)	1104.5861 ([M+2H]$^{2+}$), 744.0534 ([M+2H+Na/K]$^{3+}$)	2.0
3	1105.0653 ([M+2H]$^{2+}$),	1105.0654 ([M+2H]$^{2+}$),	-0.1
4	1080.0745 ([M+2H]$^{2+}$),	1080.0758 ([M+2H]$^{2+}$),	-1.2
5	1105.1063 ([M+2H]$^{2+}$),	1105.0651 ([M+2H]$^{2+}$),	37.3
6	1097.5776 ([M+2H]$^{2+}$),	1097.5782 ([M+2H]$^{2+}$),	-0.5
7	1068.5680 ([M+2H]$^{2+}$),	1068.5675 ([M+2H]$^{2+}$),	0.5
8	1105.0659 ([M+2H]$^{2+}$),	1105.0654 ([M+2H]$^{2+}$),	0.5
9	1097.5586 ([M+2H]$^{2+}$), 744.7065 ([M+2H+Na/K]$^{3+}$)	1097.5601 ([M+2H]$^{2+}$), 744.694 ([M+2H+Na/K]$^{3+}$)	-1.4
10	1161.6075 ([M+2H]$^{2+}$), 774.7787 ([M+3H]$^{3+}$), 782.0988 ([M+2H+Na/K]$^{3+}$)	1161.6075 ([M+2H]$^{2+}$), 774.7409 ([M+3H]$^{3+}$), 782.0678 ([M+2H+Na/K]$^{3+}$)	0.0
11	1161.6062 ([M+2H]$^{2+}$), 782.0955 ([M+2H+Na/K]$^{3+}$)	1161.6075 ([M+2H]$^{2+}$), 782.0678 ([M+2H+Na/K]$^{3+}$)	-1.1
12	1161.6080 ([M+2H]$^{2+}$),	1161.6075 ([M+2H]$^{2+}$),	0.4
13	1103.5790 ([M+2H]$^{2+}$), 736.0533 ([M+3H]$^{3+}$),	1103.5782 ([M+2H]$^{2+}$), 736.0547 ([M+3H]$^{3+}$),	0.7
14	1096.5521 ([M+2H]$^{2+}$), 1107.5481 ([M+H+Na/K]$^{2+}$), 744.0598 ([M+2H+Na/K]$^{3+}$)	1096.5521 ([M+2H]$^{2+}$), 1107.5432 ([M+H+Na/K]$^{2+}$), 743.6863 ([M+2H+Na/K]$^{3+}$)	0.0
15	1095.0654 ([M+2H]$^{2+}$), 730.4116 ([M+3H]$^{3+}$), 743.0613 ([M+2H+Na/K]$^{3+}$)	1095.0649 ([M+2H]$^{2+}$), 730.3792 ([M+3H]$^{3+}$), 743.0306 ([M+2H+Na/K]$^{3+}$)	0.5
16	1177.3290 ([M+3H]$^{3+}$), 1209.9323 ([M+Na+2K]$^{3+}$), 883.2201 ([M+4H]$^{4+}$), 907.7009 ([M+Na+2K]$^{4+}$), 706.8076 ([M+5H]$^{5+}$)	1177.3188 ([M+3H]$^{3+}$), 1209.9493 ([M+Na+2K]$^{3+}$), 883.2411 ([M+4H]$^{4+}$), 907.4648 ([M+Na+2K]$^{4+}$), 706.7944 ([M+5H]$^{5+}$)	8.7
17	1171.3730 ([M+3H]$^{3+}$), 1204.014 ([M+Na+2K]$^{3+}$), 878.7485 ([M+4H]$^{4+}$), 903.0092 ([M+Na+2K]$^{4+}$), 703.2338 ([M+5H]$^{5+}$)	1171.3274 ([M+3H]$^{3+}$), 1203.9635 ([M+Na+2K]$^{3+}$), 878.7475 ([M+4H]$^{4+}$), 902.9656 ([M+Na+2K]$^{4+}$), 703.1996 ([M+5H]$^{5+}$)	38.9
18	1176.7262 ([M+3H]$^{3+}$), 1209.3905 ([M+Na+2K]$^{3+}$), 882.4794 ([M+4H]$^{4+}$), 906.9955 ([M+Na+2K]$^{4+}$), 706.3795 ([M+5H]$^{5+}$)	1176.6470 ([M+3H]$^{3+}$), 1209.282 ([M+Na+2K]$^{3+}$), 882.7372 ([M+4H]$^{4+}$), 906.9577 ([M+Na+2K]$^{4+}$), 706.3913 ([M+5H]$^{5+}$)	67.3
19	1162.2844 ([M+3H]$^{3+}$), 1194.6675 ([M+Na+2K]$^{3+}$), 871.7327 ([M+4H]$^{4+}$), 896.0294 ([M+Na+2K]$^{4+}$),	1162.3080 ([M+3H]$^{3+}$), 1194.9363 ([M+Na+2K]$^{3+}$), 871.9829 ([M+4H]$^{4+}$), 896.2068 ([M+Na+2K]$^{4+}$),	-20.3

	697.7919 ($[M+5H]^{5+}$)	697.7879 ($[M+5H]^{5+}$)	
20	1176.0098 ($[M+3H]^{3+}$), 1208.7823 ($[M+Na+2K]^{3+}$), 882.0013 ($[M+4H]^{4+}$), 906.7006 ($[M+Na+2K]^{4+}$), 706.0279 ($[M+5H]^{5+}$)	1175.9993 ($[M+3H]^{3+}$), 1208.6347 ($[M+Na+2K]^{3+}$), 882.2515 ($[M+4H]^{4+}$), 906.472 ($[M+Na+2K]^{4+}$), 706.0027 ($[M+5H]^{5+}$)	8.9
21	1176.6498 ($[M+3H]^{3+}$), 882.4855 ($[M+4H]^{4+}$), 706.1829 ($[M+5H]^{5+}$)	1176.6470 ($[M+3H]^{3+}$), 882.7372 ($[M+4H]^{4+}$), 706.3913 ($[M+5H]^{5+}$)	2.4
22	1171.3411 ($[M+3H]^{3+}$), 1203.964 ($[M+Na+2K]^{3+}$), 878.7408 ($[M+4H]^{4+}$), 903.0154 ($[M+Na+2K]^{4+}$), 703.2175 ($[M+5H]^{5+}$)	1171.3274 ($[M+3H]^{3+}$), 1203.9635 ($[M+Na+2K]^{3+}$), 878.7475 ($[M+4H]^{4+}$), 902.9656 ($[M+Na+2K]^{4+}$), 703.1996 ($[M+5H]^{5+}$)	11.7
23	1171.6315 ($[M+3H]^{3+}$), 878.9778 ($[M+4H]^{4+}$), 703.3821 ($[M+5H]^{5+}$)	1171.6433 ($[M+3H]^{3+}$), 878.9844 ($[M+4H]^{4+}$), 703.3891 ($[M+5H]^{5+}$)	-10.1
24	1171.6426 ($[M+3H]^{3+}$), 1203.3256 ($[M+Na+2K]^{3+}$), 878.7353 ($[M+4H]^{4+}$), 902.7455 ($[M+Na+2K]^{4+}$), 703.376 ($[M+5H]^{5+}$)	1171.6433 ($[M+3H]^{3+}$), 1204.2786 ($[M+Na+2K]^{3+}$), 878.9844 ($[M+4H]^{4+}$), 903.214 ($[M+Na+2K]^{4+}$), 703.3891 ($[M+5H]^{5+}$)	-0.6
25	1195.3237 ($[M+3H]^{3+}$), 1227.6448 ($[M+Na+2K]^{3+}$), 896.493 ($[M+4H]^{4+}$), 921.4927 ($[M+Na+2K]^{4+}$), 717.6011 ($[M+5H]^{5+}$)	1195.3345 ($[M+3H]^{3+}$), 1227.9695 ($[M+Na+2K]^{3+}$), 896.7528 ($[M+4H]^{4+}$), 920.9735 ($[M+Na+2K]^{4+}$), 717.6038 ($[M+5H]^{5+}$)	-9.0
26	1162.3097 ($[M+3H]^{3+}$), 1195.3408 ($[M+Na+2K]^{3+}$), 871.737 ($[M+4H]^{4+}$), 896.2319 ($[M+Na+2K]^{4+}$), 697.7875 ($[M+5H]^{5+}$)	1162.3080 ($[M+3H]^{3+}$), 1194.9387 ($[M+Na+2K]^{3+}$), 871.9829 ($[M+4H]^{4+}$), 896.2037 ($[M+Na+2K]^{4+}$), 697.7879 ($[M+5H]^{5+}$)	1.5
27	1165.6833 ($[M+3H]^{3+}$), 874.2466 ($[M+4H]^{4+}$), 699.6055 ($[M+5H]^{5+}$)	1165.6519 ($[M+3H]^{3+}$), 874.4909 ($[M+4H]^{4+}$), 699.7943 ($[M+5H]^{5+}$)	26.9
28	1155.6561 ($[M+3H]^{3+}$), 1188.6327 ($[M+Na+2K]^{3+}$), 866.7495 ($[M+4H]^{4+}$), 891.252 ($[M+Na+2K]^{4+}$), 693.5889 ($[M+5H]^{5+}$)	1155.6447 ($[M+3H]^{3+}$), 1188.2752 ($[M+Na+2K]^{3+}$), 866.9855 ($[M+4H]^{4+}$), 891.2064 ($[M+Na+2K]^{4+}$), 693.7899 ($[M+5H]^{5+}$)	9.9
29	1155.9686 ($[M+3H]^{3+}$), 1188.6478 ($[M+Na+2K]^{3+}$), 866.9707 ($[M+4H]^{4+}$), 891.548 ($[M+Na+2K]^{4+}$), 694.149 ($[M+5H]^{5+}$)	1155.9606 ($[M+3H]^{3+}$), 1188.7028 ($[M+Na+2K]^{3+}$), 867.2224 ($[M+4H]^{4+}$), 891.527 ($[M+Na+2K]^{4+}$), 693.9794 ($[M+5H]^{5+}$)	6.9

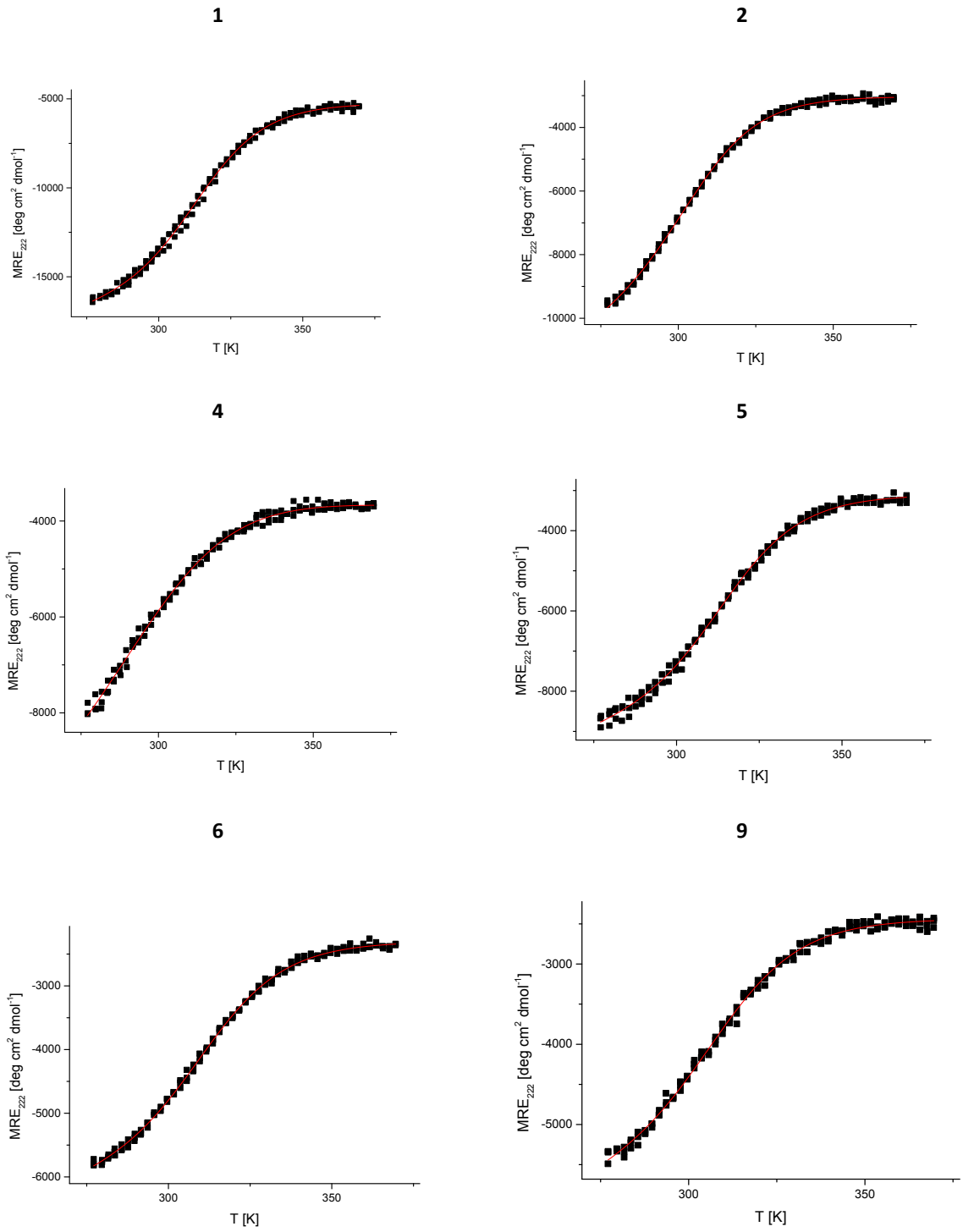

Figure S1. Plots of ellipticity (Θ_{222}) *versus* temperature (T) for peptides **1**, **2**, **4**-**6**, **9**, for which it was possible to determine T_m.

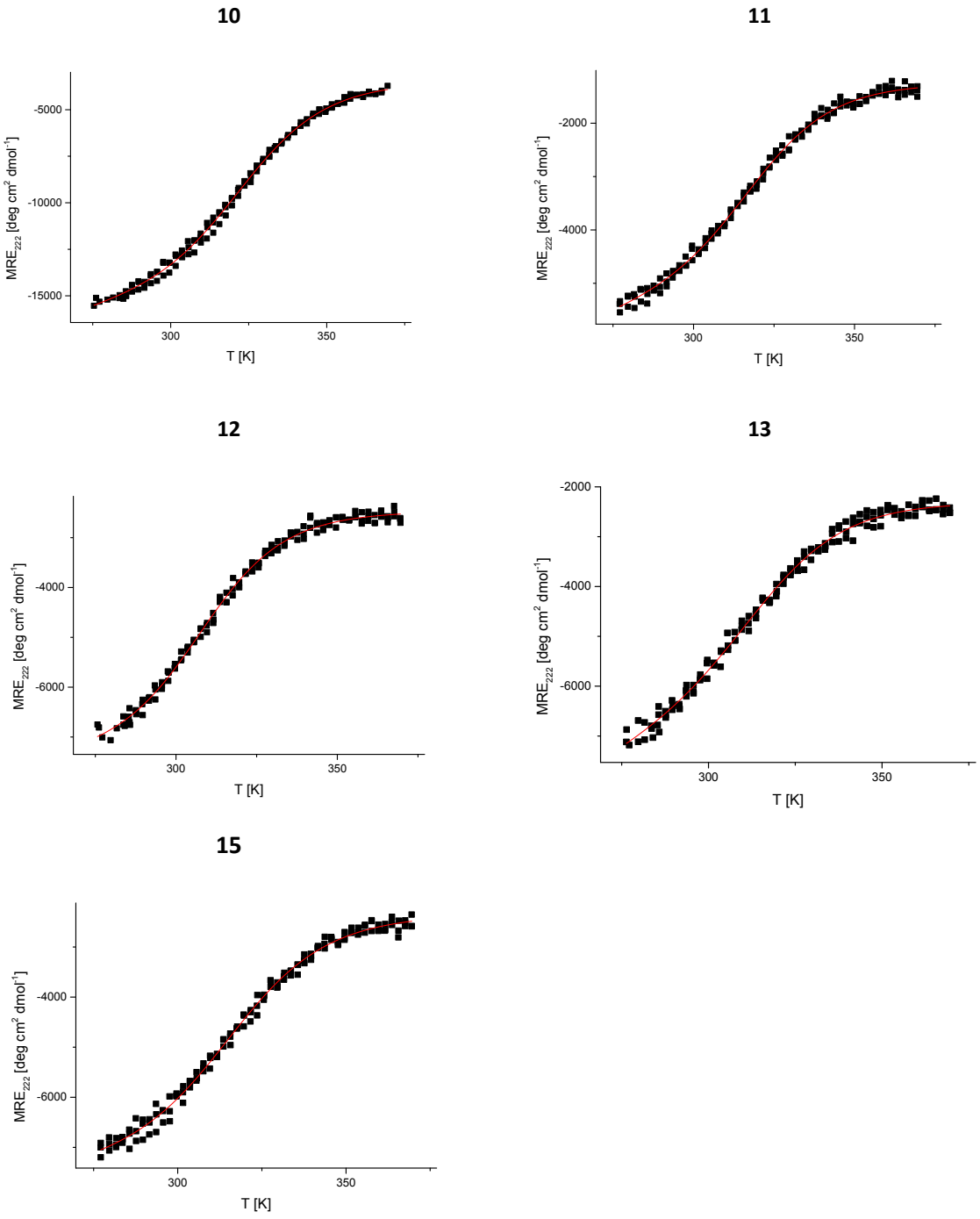

Figure S2. Plots of ellipticity (Θ_{222}) versus temperature (T) for peptides **10**, **11**-**13**, and **15**, for which it was possible to determine T_m.

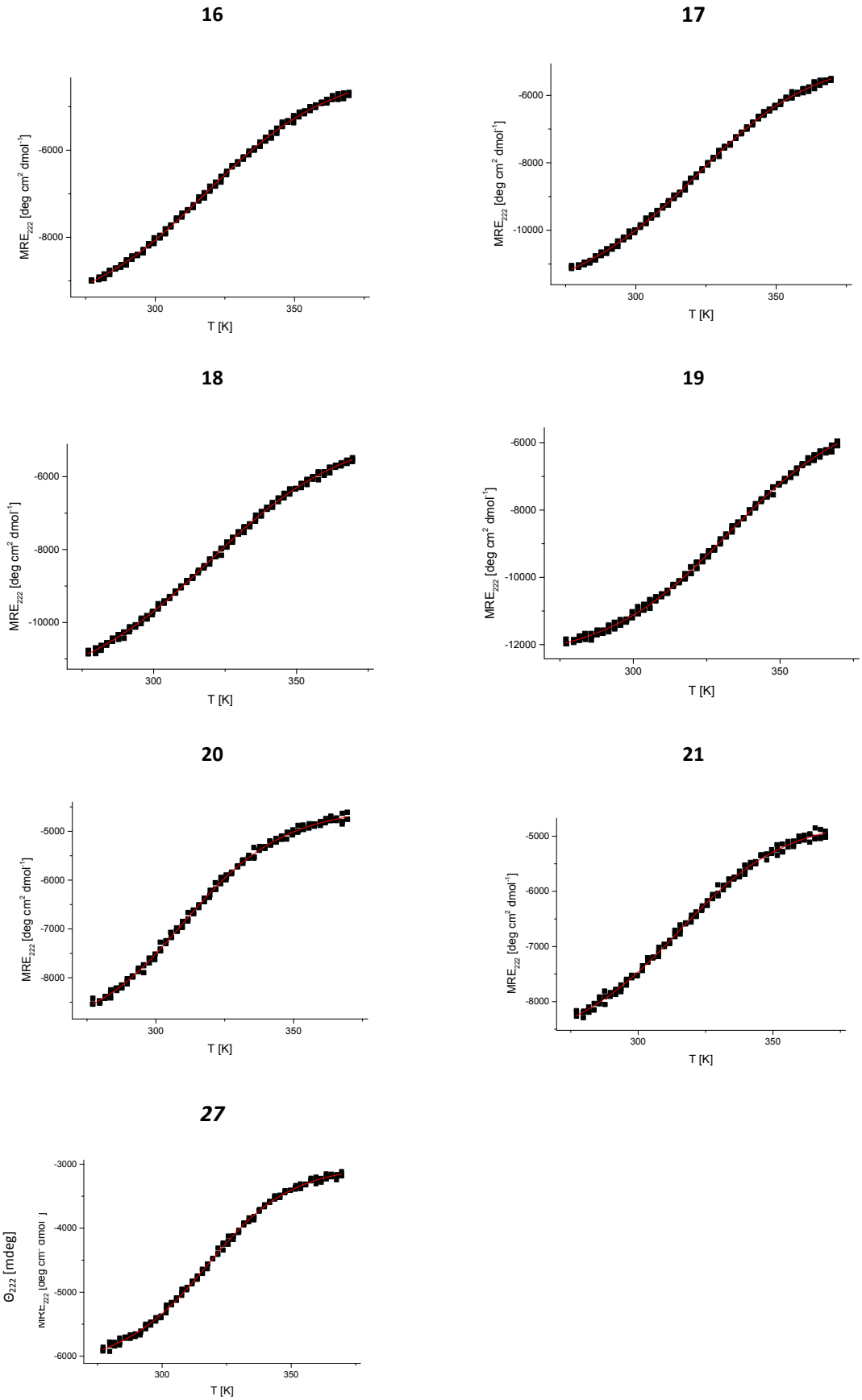

Figure S3. Plots of ellipticity (Θ_{222}) versus temperature (T) for peptides **16-21** and ***27***, for which it was possible to determine T_m.

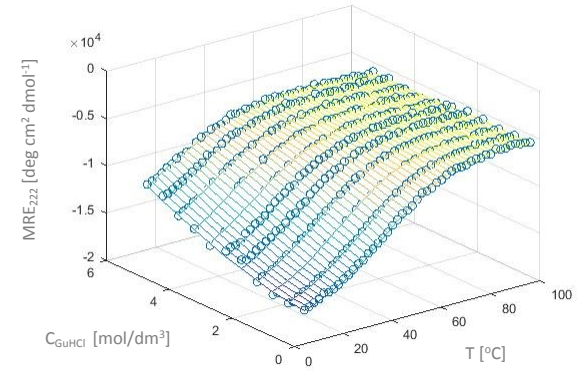

1	
ΔG°	0.30 ± 0.16 kcal/mol
ΔH°	10.6 ± 0.8 kcal/mol
TΔS°	10.1 ± 0.6 kcal/mol
ΔC_P	0.16 ± 0.03 kcal/mol·K
m	0.23 ± 0.02 kcal/mol·M
K	0.60 ± 0.16

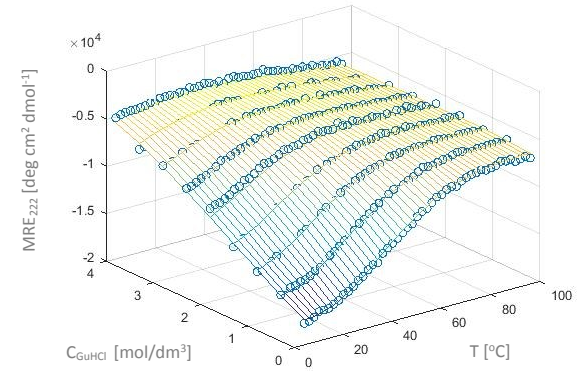

5	
ΔG°	0.48 ± 0.30 kcal/mol
ΔH°	11.7 ± 1.6 kcal/mol
TΔS°	11.3 ± 1.3 kcal/mol
ΔC_P	-0.01 ± 0.05 kcal/mol·K
m	0.40 ± 0.04 kcal/mol·M
K	0.43 ± 0.18

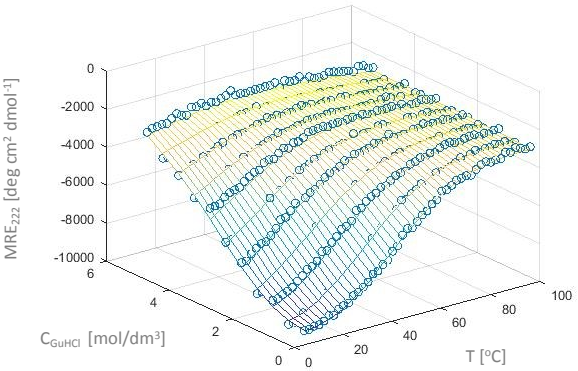

11	
ΔG°	0.28 ± 0.17 kcal/mol
ΔH°	9.6 ± 0.7 kcal/mol
TΔS°	9.3 ± 0.6 kcal/mol
ΔC_P	0.12 ± 0.03 kcal/mol·K
m	0.38 ± 0.04 kcal/mol·M
K	0.61 ± 0.14

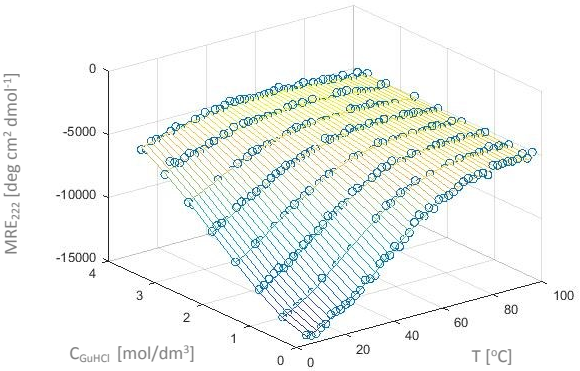

13	
ΔG°	0.24 ± 0.07 kcal/mol
ΔH°	8.4 ± 0.6 kcal/mol
TΔS°	8.2 ± 0.6 kcal/mol
ΔC_P	0.14 ± 0.03 kcal/mol·K
m	0.44 ± 0.05 kcal/mol·M
K	0.66 ± 0.10

Figure S4. CD signal at 222nm monitored in a function of guanidine hydrochloride concentration and temperature for peptide **1**, **5**, **11**, and **13** (experimental data are shown as dark green circles, while fitted thermodynamic parameters for the folding equilibrium are represented by the surface). Values of ΔG^o, $T\Delta S$ and K are given for 293K.

Table S3. Chemical shifts of peptide **13** in 50mM phosphate buffer, pH 7. Cp stands for *trans*-(1*S,*2*S*)-2-amino-1-cyclopentanecarboxylic acid. Residue no 1 is acetyl group at *N*-terminus.

Residue	Proton	Chemical shift [ppm]
Ac 1	HA	1.81
Cp2	HN	8.10
	HA	2.48
	HB	3.98
	HG,HD,HE	1.45(4) 1.52(3) 1.55(2) 1.85(1)
Leu3	HN	8.27
	HA	3.91
	HB	1.43
	HG	1.17
	HD	0.61(2) 0.69(1)
Tyr4	HN	8.10
	HA	4.06
	HB	2.80(2) 3.05(1)
	HD	6.79
	HE	6.53
Cp5	HN	8.08
	HA	2.38
	HB	4.05
	HG,HD,HE	1.40(5) 1.53(4) 1.65(3) 1.76(2) 1.88(1)
Gln6	HN	7.93
	HA	3.61
	HB	1.86(2), 1.91(1)
	HG	2.12
	HN’	6.67(2) 7.37(1)
Trp7	HN	7.81
	HA	4.14
	HB	2.96(2) 3.59(1)
	HD1	6.83
	HE3	6.87
	HH2	6.92
	HZ2	7.00
	HZ3	6.82
	HE1	9.48
Leu8	HN	8.20
	HA	3.19
	HB	1.42(2) 1.51(1)
	HG	1.13
	HD	0.61(2) 0.69(1)
Cp9	HN	8.19
	HA	2.57
	HB	3.89
	HG,HD,HE	1.45(3) 1.65(2) 1.71(1)
Asp10	HN	7.96
	HA	4.23
	HB	2.57(2) 2.64(1)
Gly11	HN	7.05
	HA	3.26(2) 3.85(1)
Gly12	HN	8.50
	HA	0.80(1) 2.99(2)
Pro13	HA	4.34
	HB	2.23(1) 1.82(2)
	HG	1.90
	HD	3.22(2) 3,55(1)
Ser14	HN	7.59
	HA	4.17
	HB	3.66(2) 3.68(1)
Ser15	HN	8.02
	HA	3.93
	HB	3.38(2) 3.65(1)
Gly16	HN	7.71
	HA	3.61(2) 3.98(1)
Arg17	HN	8.00
	HA	4.70
	HB	1.58(2) 1.64(1)
	HG	1.42
	HD	3.02
	HN’	6.83(2)

		7.34(1)
Pro18	HA	4.49
	HB	2.09(1), 1.56(2)
	HG	1.76
	HD	3.42(2) 3.62(1)
Pro19	HA	3.26
	HB	0.21(2) 1.09(1)
	HG	1.40(2) 1.50(1)

	HD	2.53
Pro20	HA	4.12
	HB	2.00
	HG	1.66
	HD	2.78(2) 3.03(1)
Ser21	HN	8.05
	HA	4.07
	HB	3.56(2) 3.60(1)
NH_2	HN1	6.91
	HN2	7.42

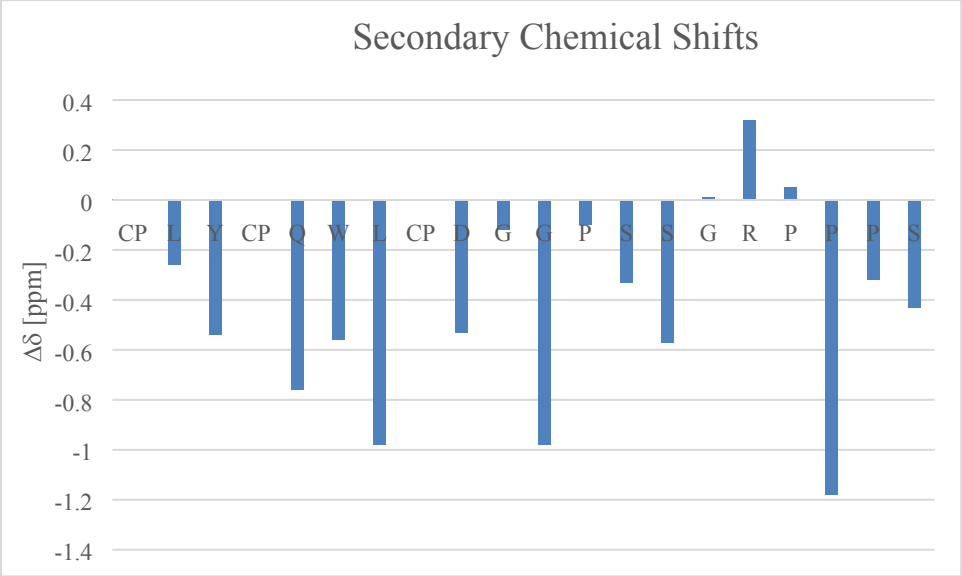

Figure S5. Differences between ^{1}H chemical shifts of HA protons of peptide **13** and random coil shifts for specific amino acid residues.

Table S4. Interproton contacts of peptide **13** in 50mM phosphate buffer, pH 7**.** Cp stands for *trans*-(1*S,*2*S*)-2-amino-1-cyclopentanecarboxylic acid. Residue no 1 is acetyl group at *N*-terminus.

Sequential (*i*, *i*+1)	**Intensity**
Ac1CH_3-Cp2HN	s
Cp2$CH_2$1-L3HN	m
Cp2$CH_2$3-L3HN	m
Cp2HA-L3HA	m
Cp2HA-L3HN	s
Cp2HB-L3HN	m
Cp2HN-L3HG	m
L3HA-Y4HN	s
L3HB-Y4HE	m
L3HD1-Y4HD	m
L3HD1-Y4HE	m
L3HD1-Y4HN	m
L3HD2-Y4HD	s
L3HD2-Y4HE	m
L3HD2-Y4HN	m
L3HN-Y4HA	w
L3HN-Y4HN	m
Y4HA-Cp5HN	s
Y4HB1-Cp5HN	s
Y4HB2-Cp5HN	s
Y4HD-Cp5HN	m
Y4HD-Cp5$CH_2$1	m
Y4HD-Cp5$CH_2$2	w
Y4HD-Cp5$CH_2$3	s
Y4HE-Cp5$CH_2$1	w
Y4HE-Cp5$CH_2$2	s
Y4HN-Cp5CH_2	s
Cp5$CH_2$2-Q6HN	s
Cp5$CH_2$3-Q6HN'1	m
Cp5HN-Q6HN	s
Cp5HA-Q6HN	s
Cp5HB-Q6HN	m
Q6HA-W7HN	s
Q6HB1-W7HN	s
Q6HB2-W7HN	s
Q6HG-W7HN	m
Q6HN-W7HN	m
W7HA-L8HN	m
W7HB1-L8HN	s
W7HB2-L8HN	m
W7HE3-L8HG	w
W7HE3-L8HA	m
W7HE3-L8HB1	m
W7HE3-L8HD1	m
W7HE3-L8HD2	m
W7HE3-L8HN	m
W7HH2-L8HD2	w
W7HH2-L8HD1	m
W7HN-L8HB2	m
W7HN-L8HN	m
W7HZ3-L8HD1	s
W7HZ3-L8HN	m
W7HZ3-L8HD2	m
W7HZ2-L8HD1	w
W7HZ2-L8HD2	w
L8HA-Cp9HN	s
L8HB1-Cp9HB	s
Cp9HN-D10HN	m
Cp9$CH_2$2-D10HN	s
Cp9$CH_2$3-D10HN	m
Cp9HA-D10HN	m
Cp9HA-D10HB2	w
Cp9HB-D10HN	s
D10HA-G11HN	m
D10HN-G11HN	m
G11HA1-G12HN	m
G11HA2-G12HN	m
G11HN-G12HN	s
G12HA1-P13HD2	s
G12HA2-P13HD2	m
G12HN-P13HD1	w
P13HA-S14HN	w
P13HD1-S14HN	w
S14HA-S15HN	m
S14HN-S15HN	m
S15HA-G16HN	s
G16HA1-R17HN	s
G16HA2-R17HN	s
G16HN-R17HN	s
G16HN-R17HA	m
R17HB1-P18HD1	s
R17HB1-P18HD2	s
P18HB1-P19HA	s
P18HG-P19HA	m
P18HB2-P19HA	s
P18HA-P19HA	w
P19HB2-P20HD2	w
P20HA-S21HN	s
P20HG-S21HN	s
S21HA-NH2HN2	m
Medium range (*i*, *i*+2)	**Intensity**
Cp2$CH_2$3-Y4HE	s
L3HN-Cp5$CH_2$1	w
Y4HD-Q6HB1	w
Cp5HB-W7HZ1	m
Cp5HB-W7HZ3	m
W7HA-Cp9HA	s
P13HA-S15HN	m
S14HA-G16HN	m
S15HN-R17HA	s
Medium range (*i*, *i*+3)	**Intensity**
Ac1HA-Y4HB1	m
Ac1HA-Y4HD	m
Ac1HA-Y4HE	w
Cp2HB-Cp5$CH_2$2	m
Cp2HB-Cp5HA	s
L3HA-Q6HB1	s
L3HA-Q6HN	s
L3HB-Q6HA	m
L3HA-Q6HB2	s
L3HA-Q6HG	m
Y4HA-W7HE3	m
Y4HA-W7HN	m
Y4HA-W7HB2	s
Cp5HB-L8HN	s
Cp5HB-L8HD1	s
Cp5HB-L8HD2	m
Cp5HB-L8HG	m
Q6HA-Cp9HN	s
Q6HN'2-Cp9HA	m
Q6HA-Cp9HA	m
W7HA-D10HN	m
W7HA-D10HB1	w
L8HA-G11HN	s
G12HN-S15HB1	m
G12HN-S15HB2	m
S14HN-R17HA	m
R17HA-P20HD2	s
P19HA-NH_2HN1	s

Medium range (*i*, *i*+4)	Intensity
Cp2CH$_2$3-Q6HN	m
Cp2HB-Q6HN	m
L3HA-W7HN	m
L8HA-G12HN	s
L8HD1-G12HN	w
L8HD2-G12HN	m
G11HA-S15HN	w

Long range (*i*, *i*>4)	Intensity
Y4HD-P19HB1	m
Y4HE-P19HB1	s
Y4HE-P19HB2	w
W7HA-G12HN	w
W7HH2-P13HA	m
W7HZ2-P13HA	s
W7HH2-P13HD1	w
W7HH2-P13HD2	m
W7HZ3-P13HD2	m
W7HZ2-P13HD2	s
W7HH2-P13HG	s
W7HZ2-P13HG	m
W7HH2-P13HB2	w
W7HZ2-P13HB2	w
W7HZ2- P19HA	m
W7HZ2 – P19HG1	w
W7HN-P20HD1	w

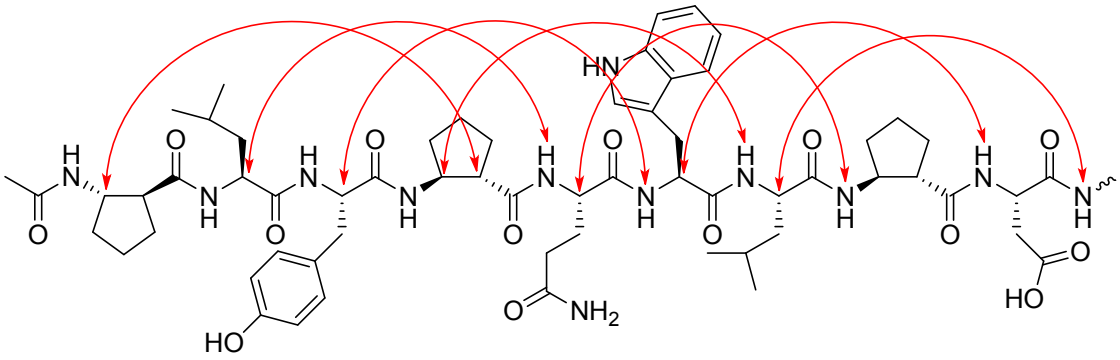

Figure S6. NOE *i* – (*i* + 3) contacts of N-terminal helix of peptide **13**.

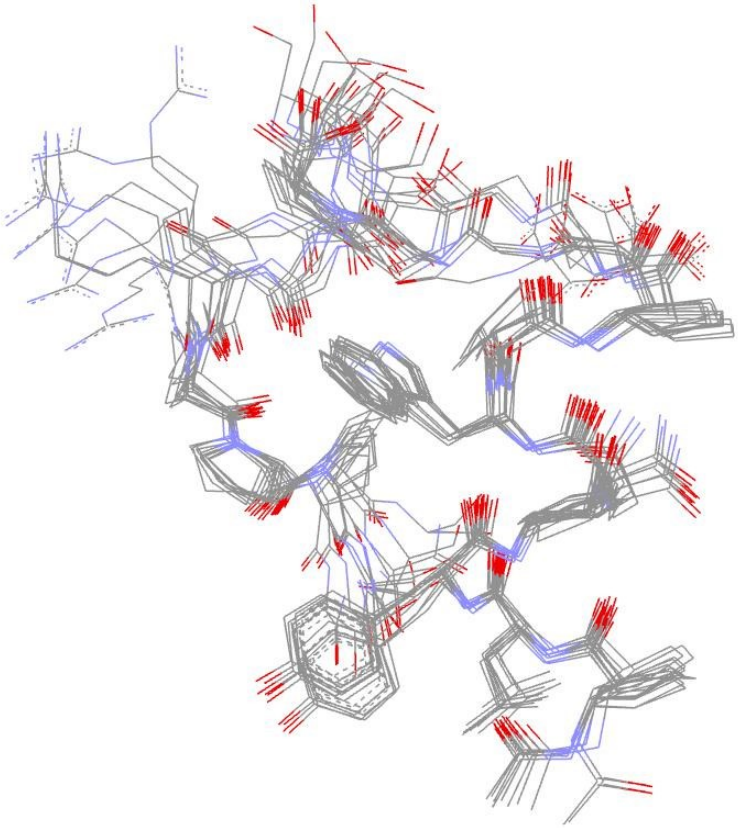

Figure S7. Superimposition of 10 lowest energy structures of peptide **13** obtained during molecular dynamics with NMR constraints.

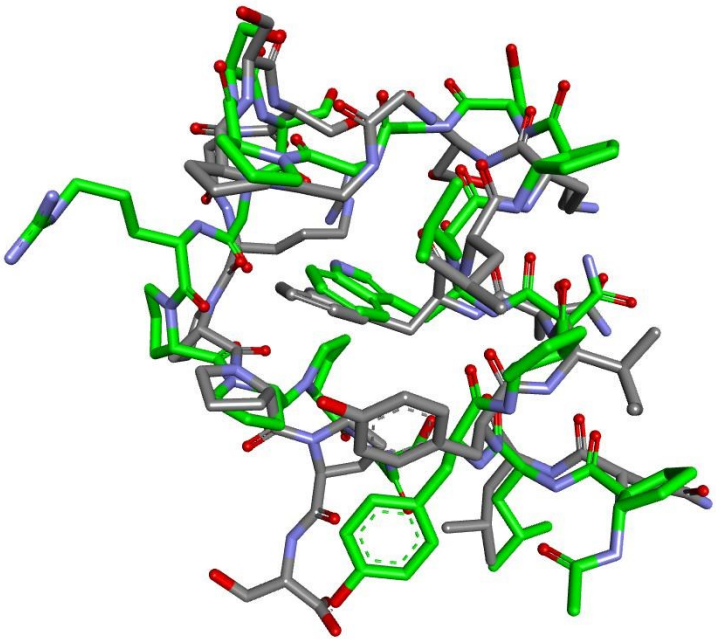

Figure S8. superimposition of average NMR (green carbon atoms) structure of peptide **13** and native Trp-cage (PDB id 1L2Y, grey carbon atoms).

Table S5. Statistics of NMR structure calculation

NOE restraints	
Total	135
Sequential ($\|i-j\| = 1$)	77
Medium ($1 < \|i-j\| \leq 4$)	41
long range ($\|i-j\| > 4$)	17
Average number of NOE violations	1.2
Average sum of upper limit violations	0.68 Å
Average sum of VdW violations	0.68 Å
Average RMDS (backbone)	0.75 Å

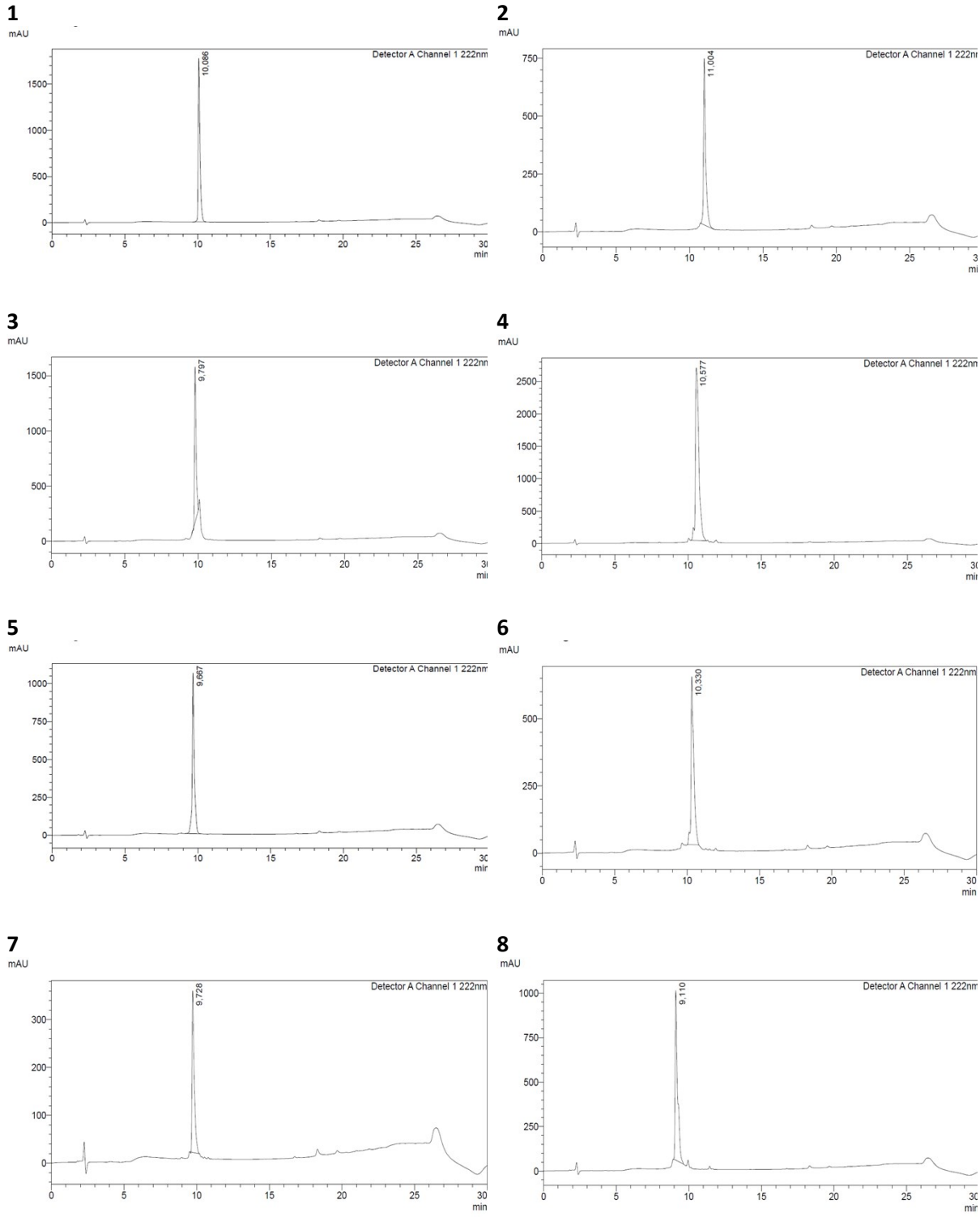

Figure S9. Analytical chromatograms for peptides **1-29**.

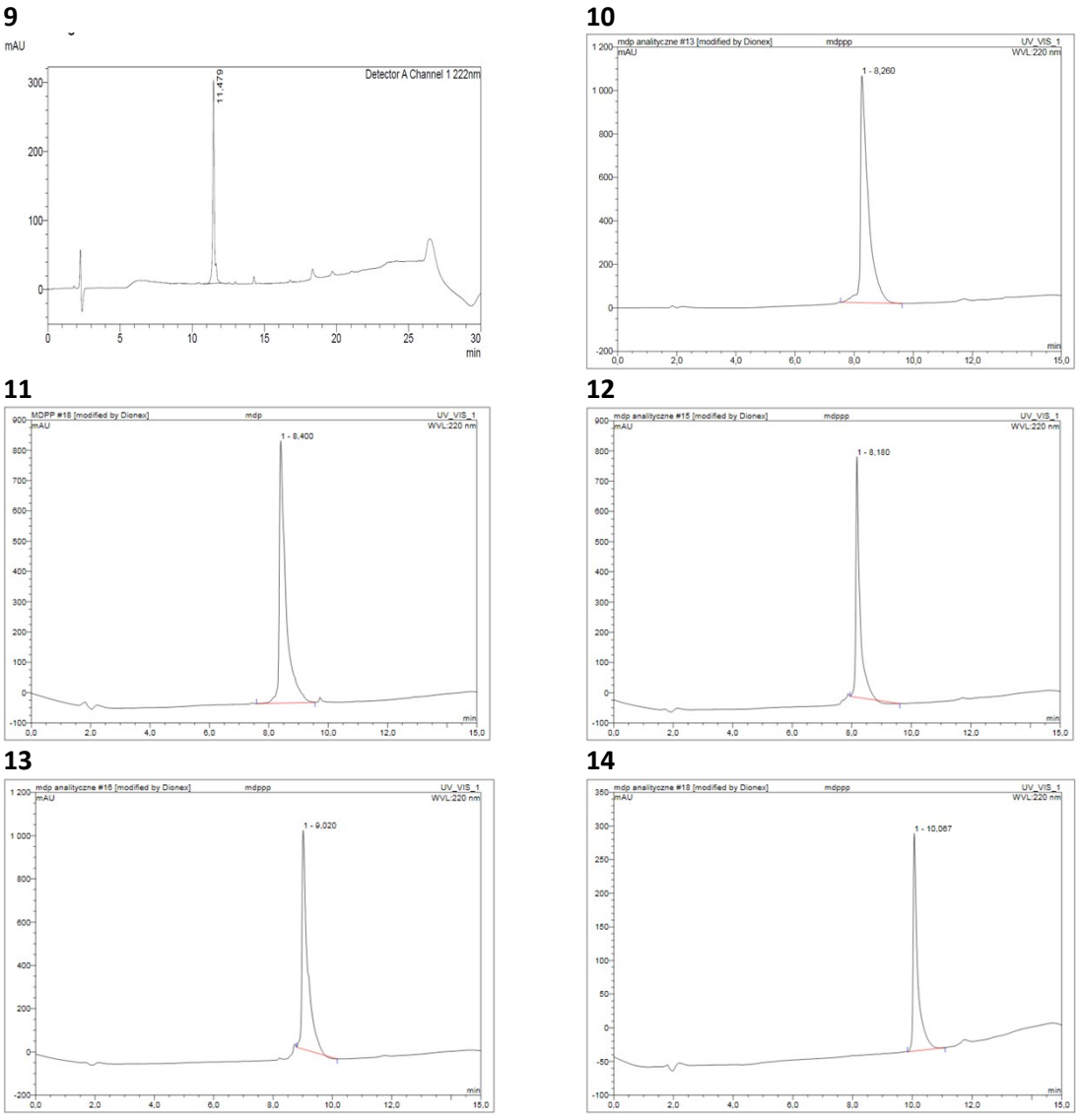

Figure S9 (continued). Analytical chromatograms for peptides **1-29**.

15

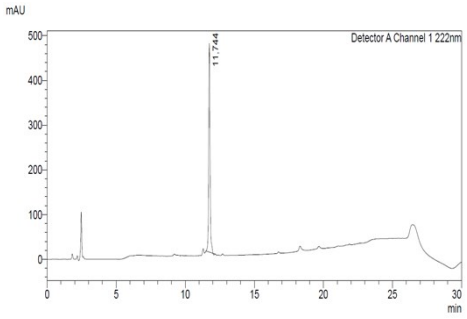

16

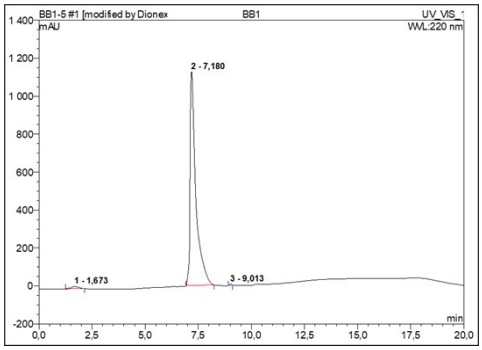

17

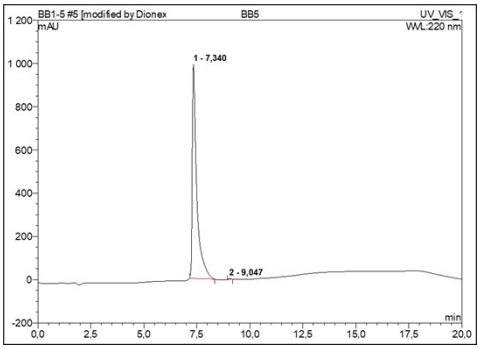

18

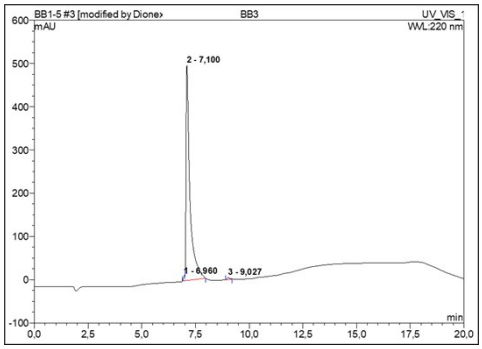

19

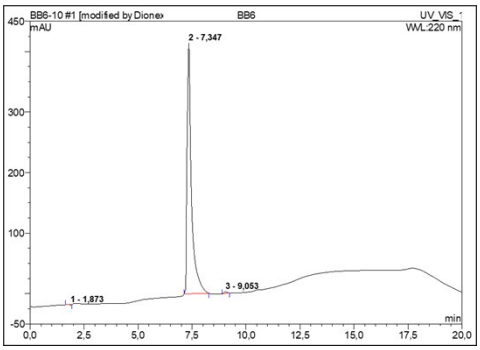

20

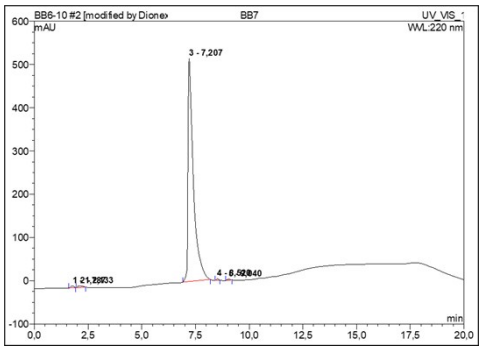

21

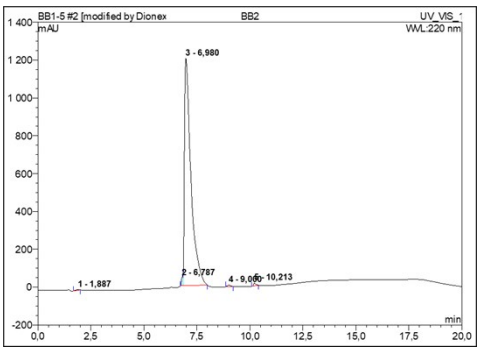

22

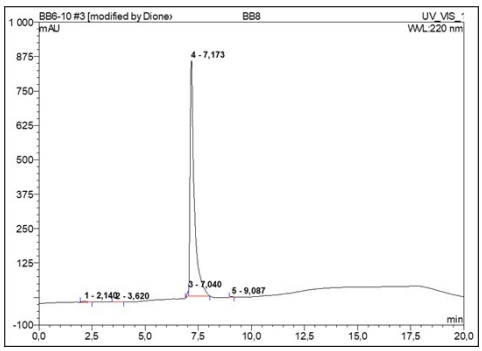

Figure S9 (continued). Analytical chromatograms for peptides **1-29**.

23

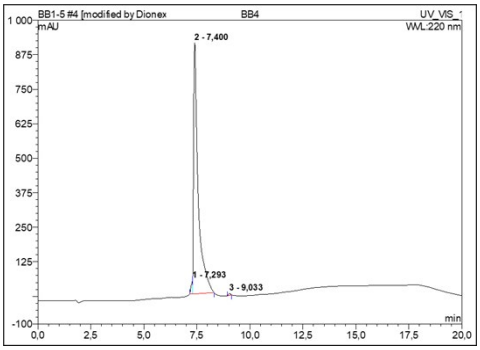

24

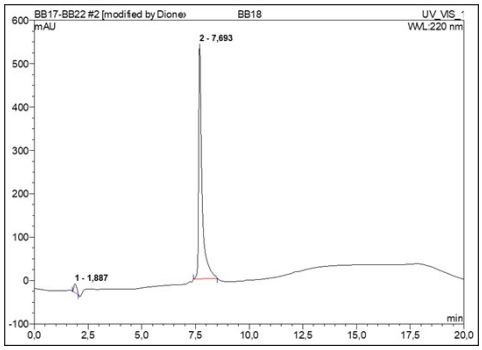

25

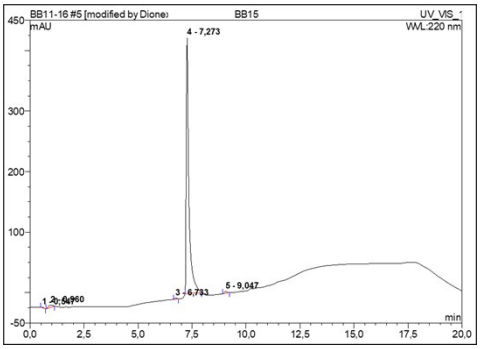

26

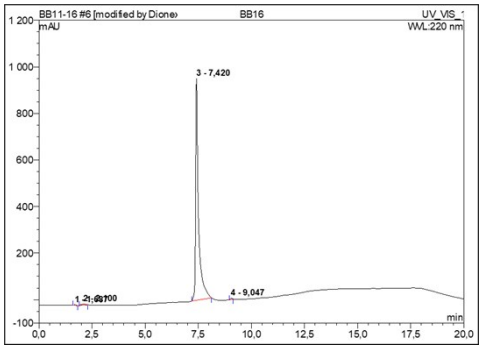

27

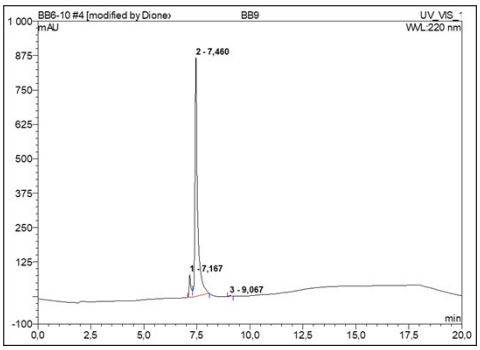

29

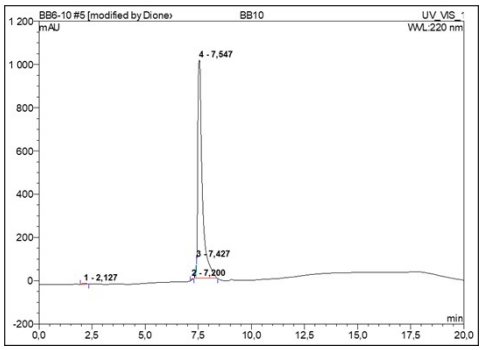

Figure S9 (continued). Analytical chromatograms for peptides **1-29**.

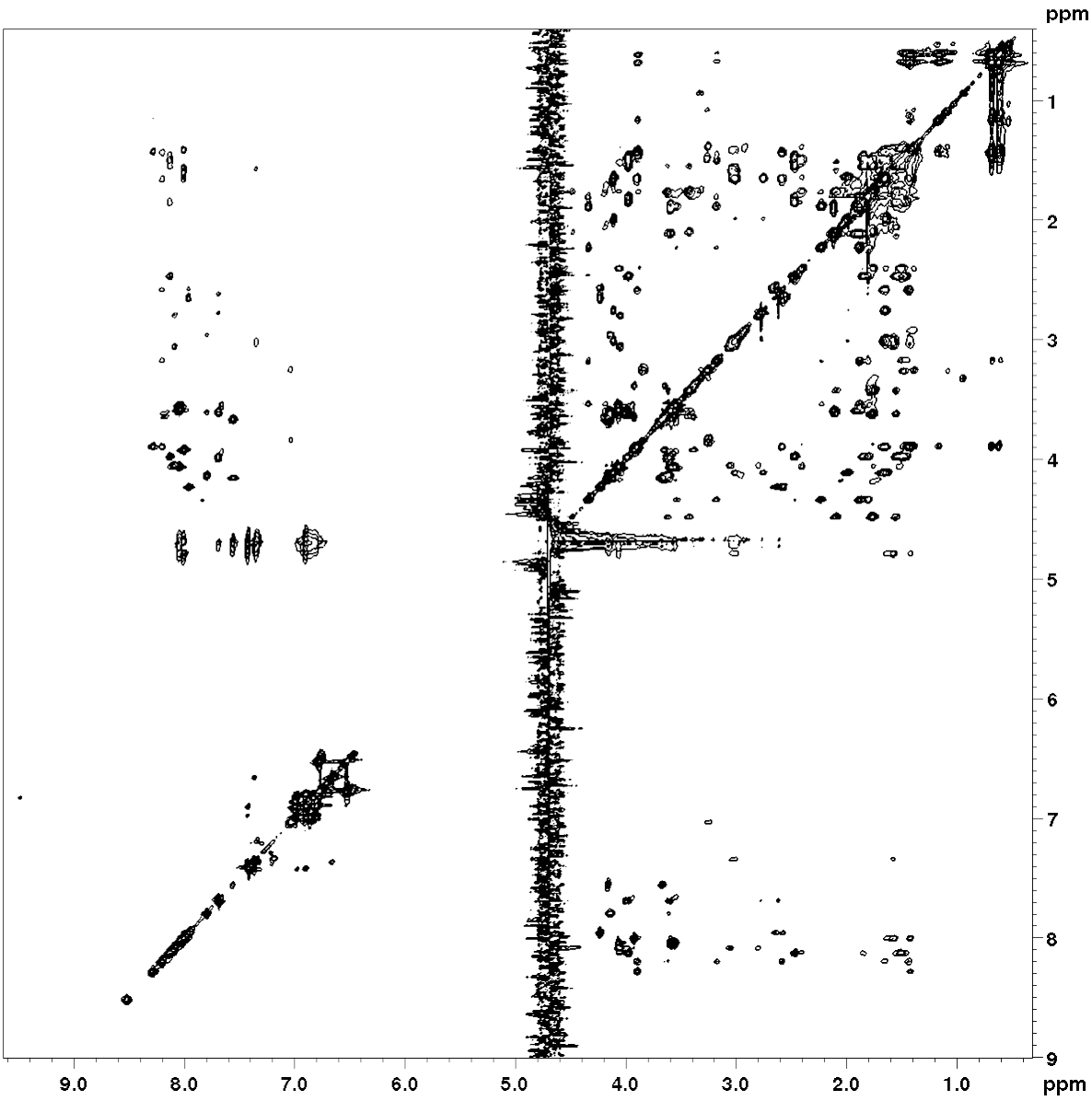

Figure S10. 2D TOCSY spectrum of peptide **13** dissolved in phosphate buffer 7.0 (10% D_2O) measured at 285K.

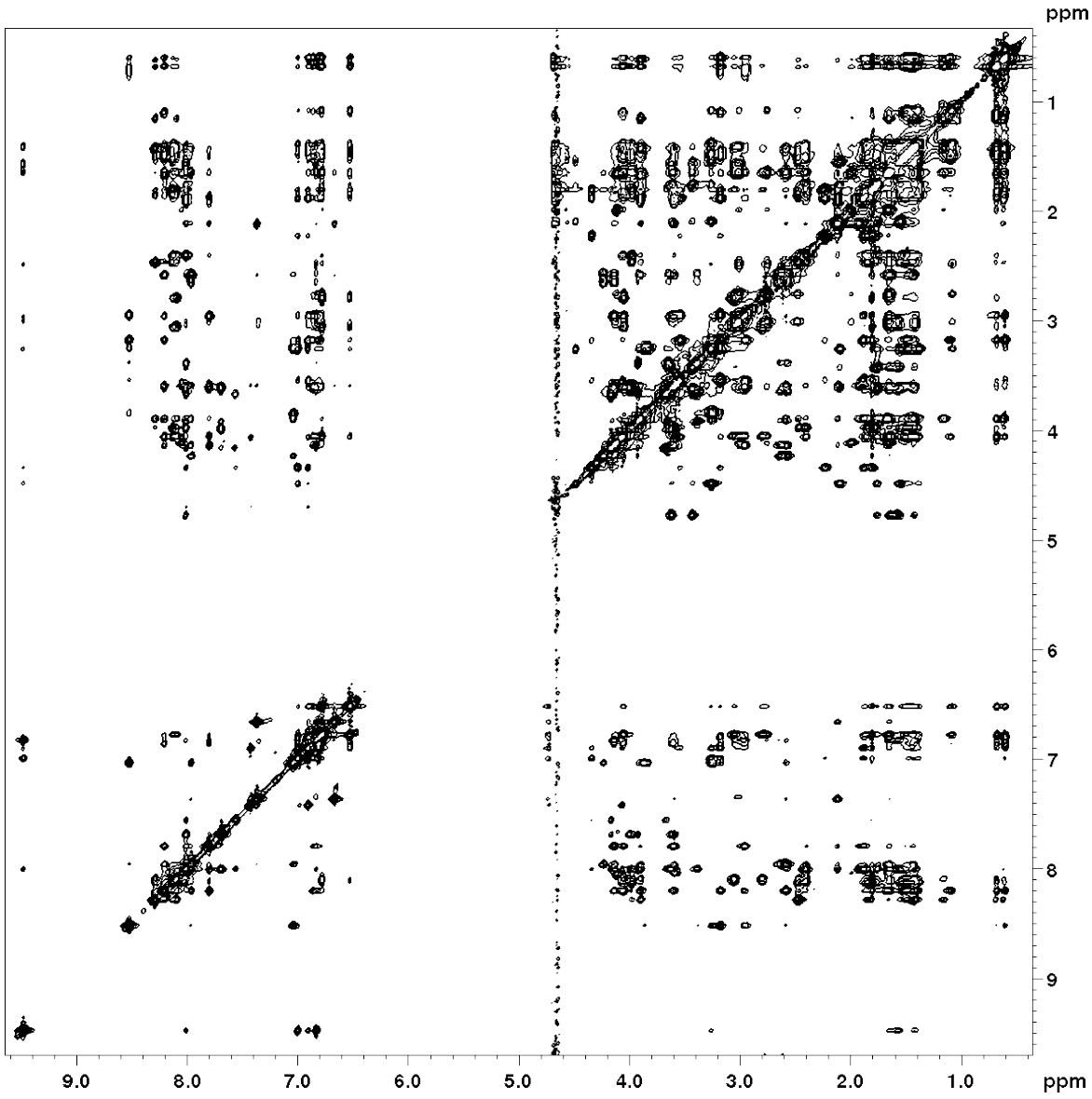

Figure S11. 2D NOESY spectrum of peptide **13** dissolved in phosphate buffer 7.0 (10% D_2O) measured at 285K.

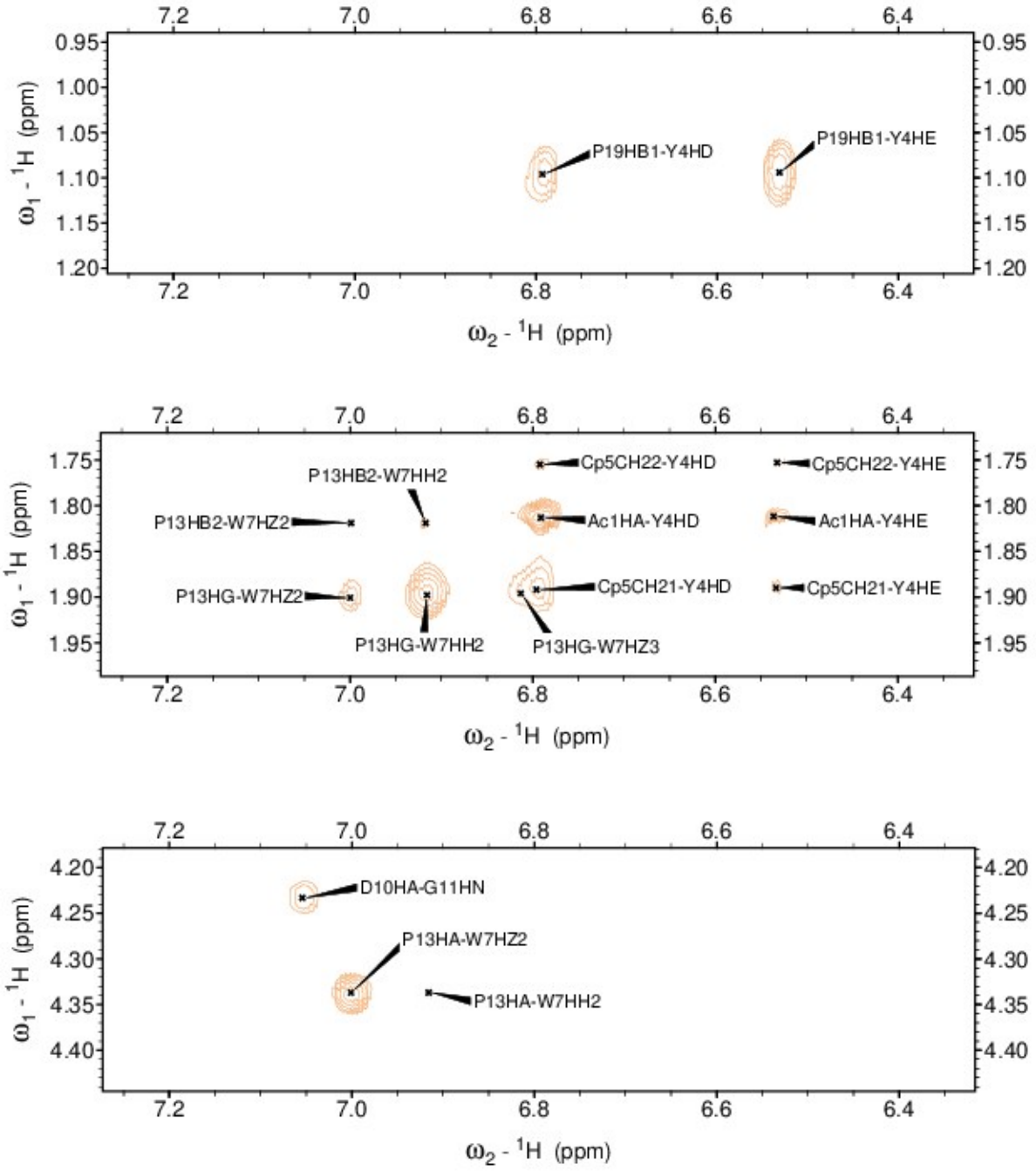

Figure S12. Annotated fragments of NOESY spectrum (phosphate buffer pH 7, 10% D_2O, 285K) of peptide **13** including long range inter-proton contacts.

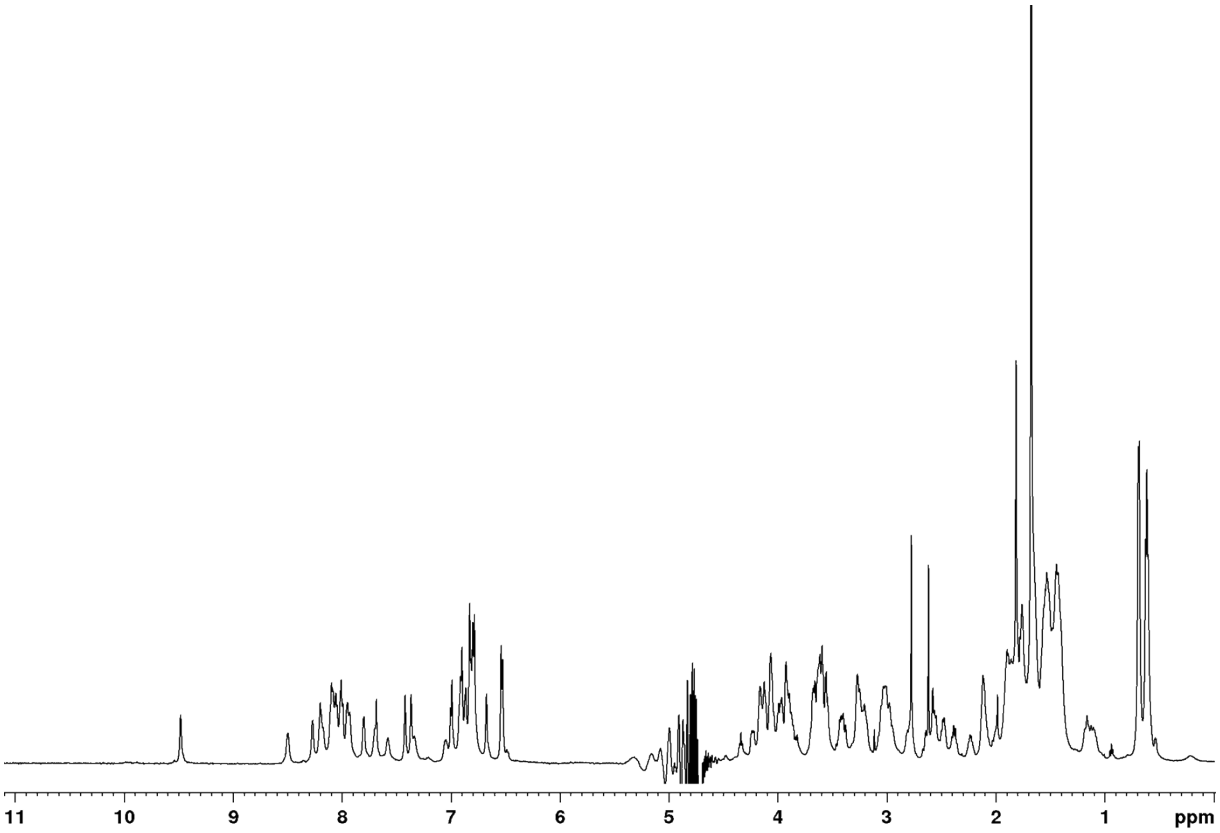

Figure S13. ^{1}H NMR spectrum of peptide **13** dissolved in phosphate buffer 7.0 (10% D_2O) measured at 285K.

References

S1. D. F. Kreitler, D. E. Mortenson, K. T. Forest, and S. H Gellman, *J. Am. Chem. Soc.* **2016**, *138*, 6498-6505.
S2. Z. E. Reinert Z. E., and W. S. Horne, *Chem. Sci.* **2014**, *5*, 3325-3330.

1

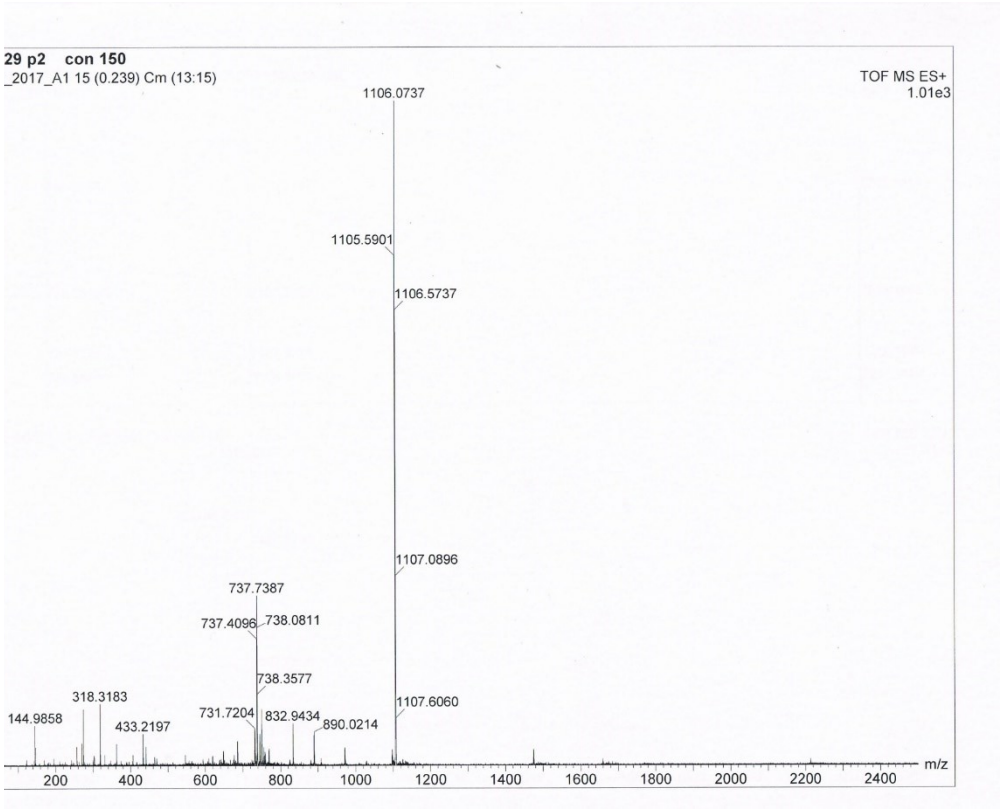
29 p2 con 150
_2017_A1 15 (0.239) Cm (13:15)
TOF MS ES+
1.01e3
1106.0737
1105.5901
1106.5737
1107.0896
737.7387
737.4096
738.0811
738.3577
318.3183
144.9858
433.2197
731.7204
832.9434
890.0214
1107.6060
m/z
200
400
600
800
1000
1200
1400
1600
1800
2000
2200
2400

2

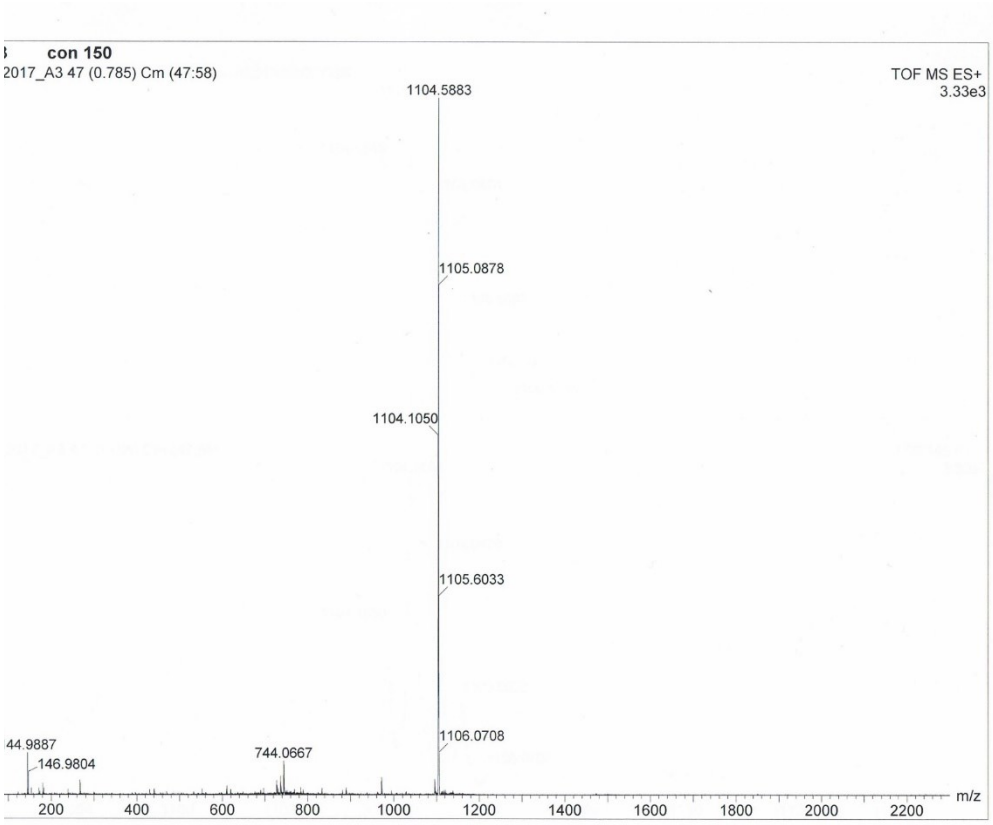
con 150
2017_A3 47 (0.785) Cm (47:58)
TOF MS ES+
3.33e3
1104.5883
1105.0878
1104.1050
1105.6033
1106.0708
744.0667
146.9804
44.9887
m/z
200
400
600
800
1000
1200
1400
1600
1800
2000
2200

3

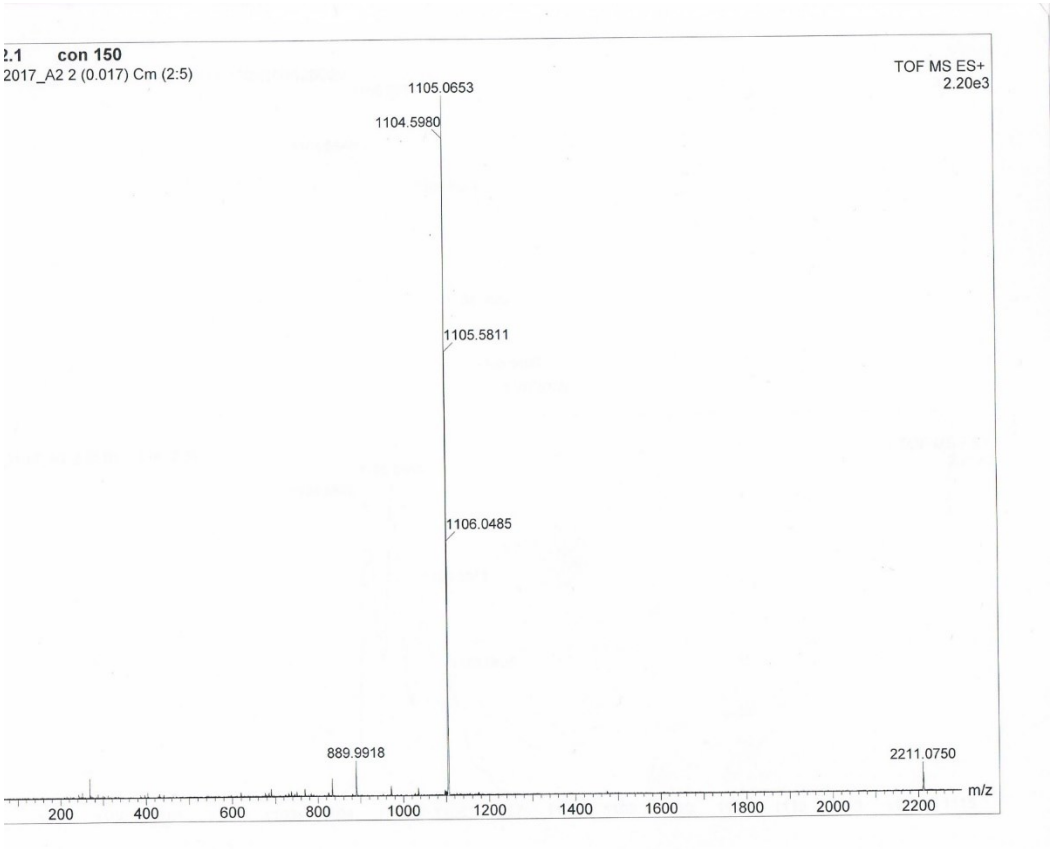
2.1 con 150
2017_A2 2 (0.017) Cm (2:5)
TOF MS ES+
2.20e3
1105.0653
1104.5980
1105.5811
1106.0485
889.9918
2211.0750
m/z
200
400
600
800
1000
1200
1400
1600
1800
2000
2200

4

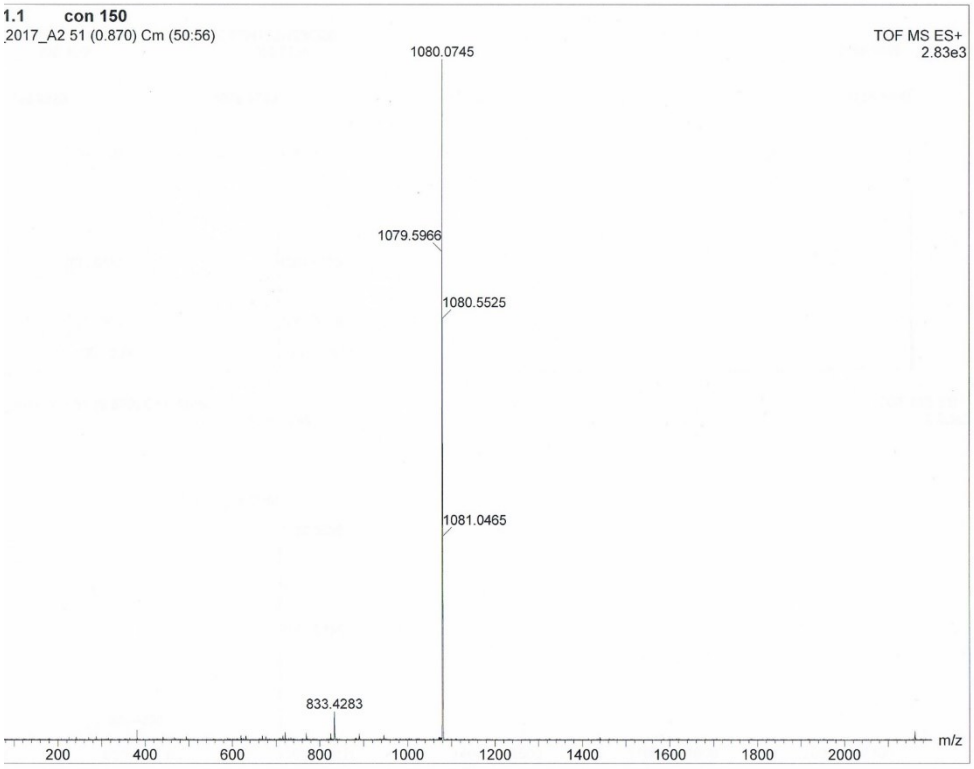
1.1 con 150
2017_A2 51 (0.870) Cm (50:56)
TOF MS ES+
2.83e3
1080.0745
1079.5966
1080.5525
1081.0465
833.4283
200
400
600
800
1000
1200
1400
1600
1800
2000
m/z

5

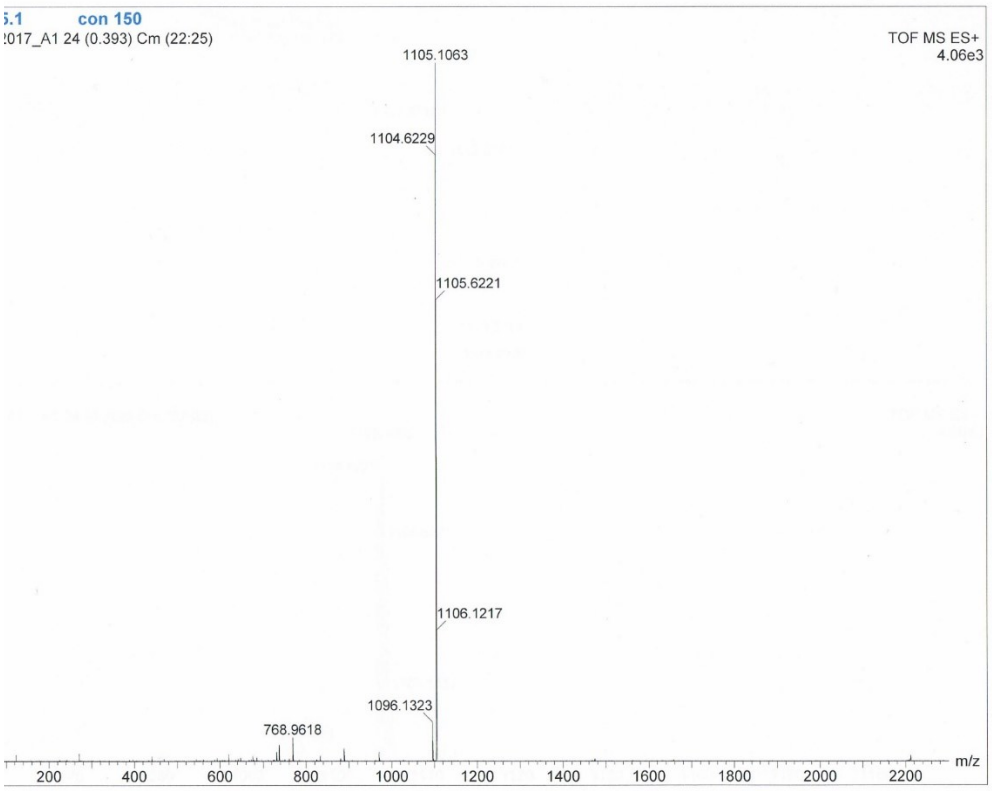
5.1 con 150
2017_A1 24 (0.393) Cm (22:25)
TOF MS ES+
4.06e3
1105.1063
1104.6229
1105.6221
1106.1217
1096.1323
768.9618
200
400
600
800
1000
1200
1400
1600
1800
2000
2200
m/z

6

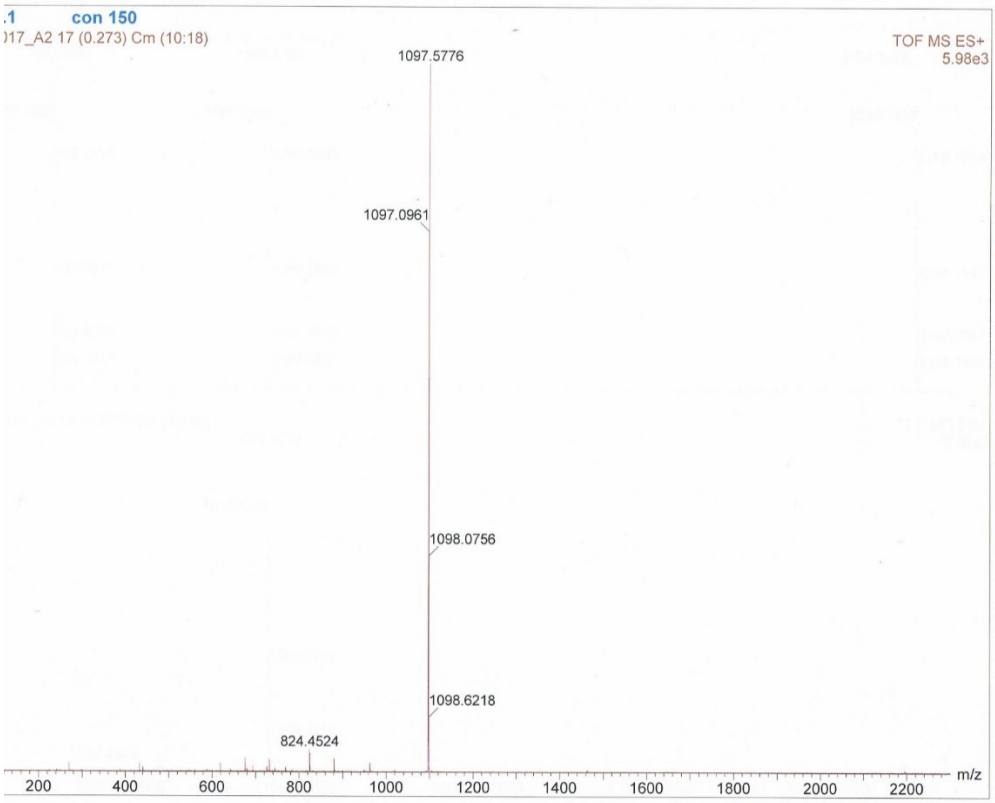
.1 con 150
)17_A2 17 (0.273) Cm (10:18)
TOF MS ES+
5.98e3
1097.5776
1097.0961
1098.0756
1098.6218
824.4524
200
400
600
800
1000
1200
1400
1600
1800
2000
2200
m/z

7

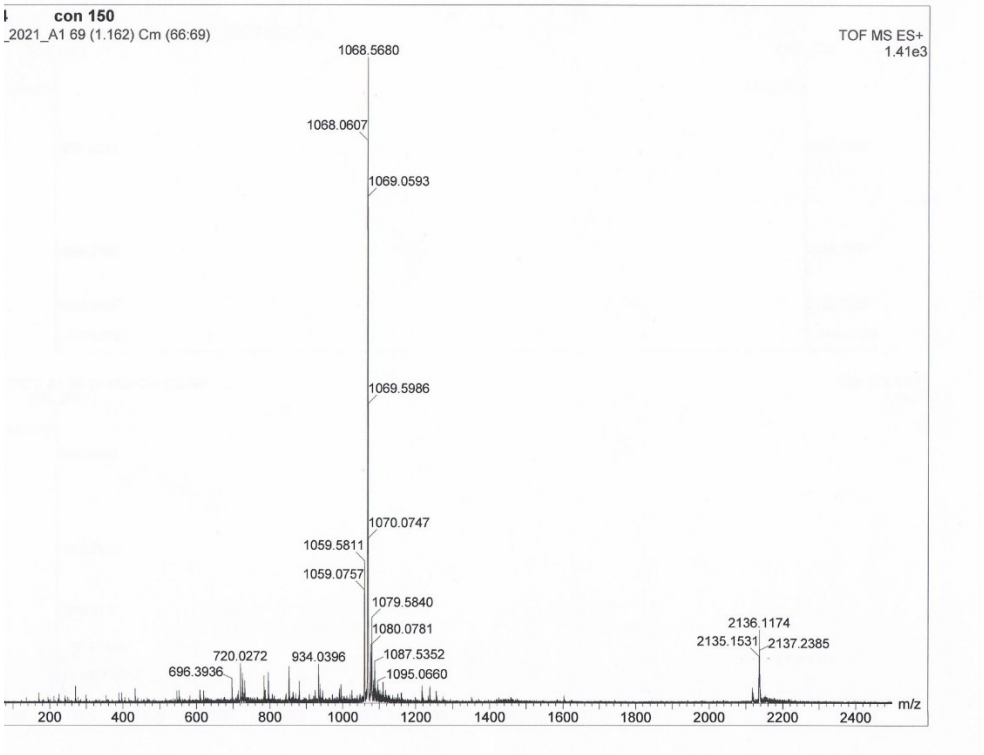
con 150
_2021_A1 69 (1.162) Cm (66:69)
TOF MS ES+
1.41e3
1068.5680
1068.0607
1069.0593
1069.5986
1070.0747
1059.5811
1059.0757
1079.5840
1080.0781
1087.5352
1095.0660
720.0272
934.0396
696.3936
2136.1174
2135.1531
2137.2385
m/z
200
400
600
800
1000
1200
1400
1600
1800
2000
2200
2400

8

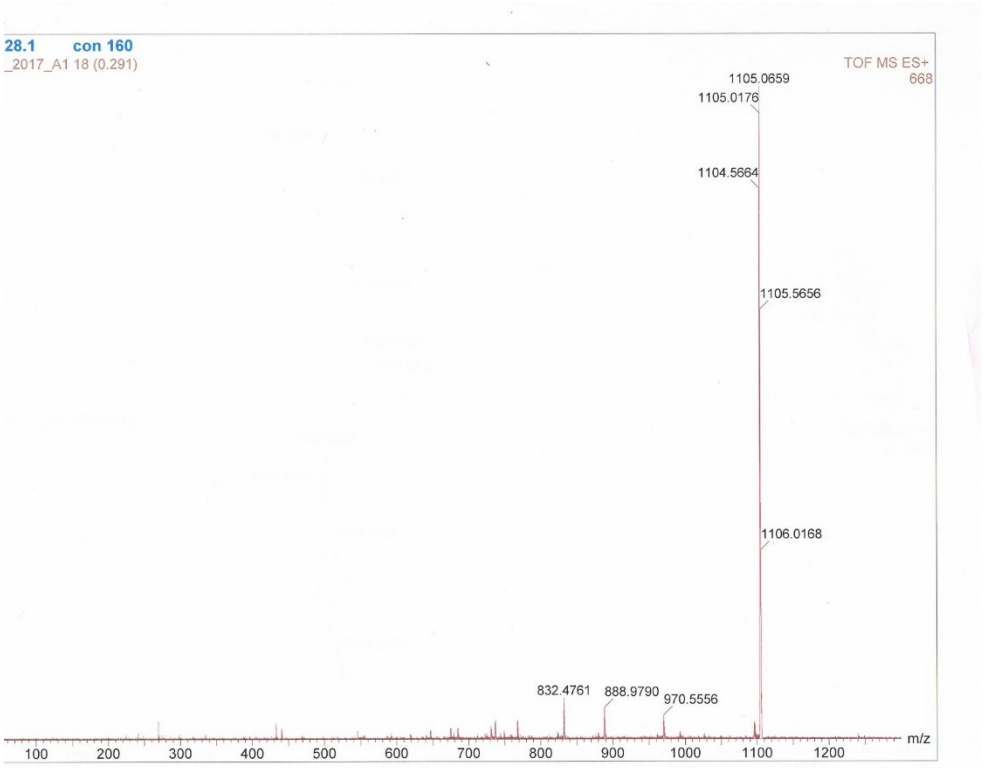
28.1 con 160
_2017_A1 18 (0.291)
TOF MS ES+
668
1105.0659
1105.0176
1104.5664
1105.5656
1106.0168
832.4761
888.9790
970.5556
m/z
100
200
300
400
500
600
700
800
900
1000
1100
1200

9

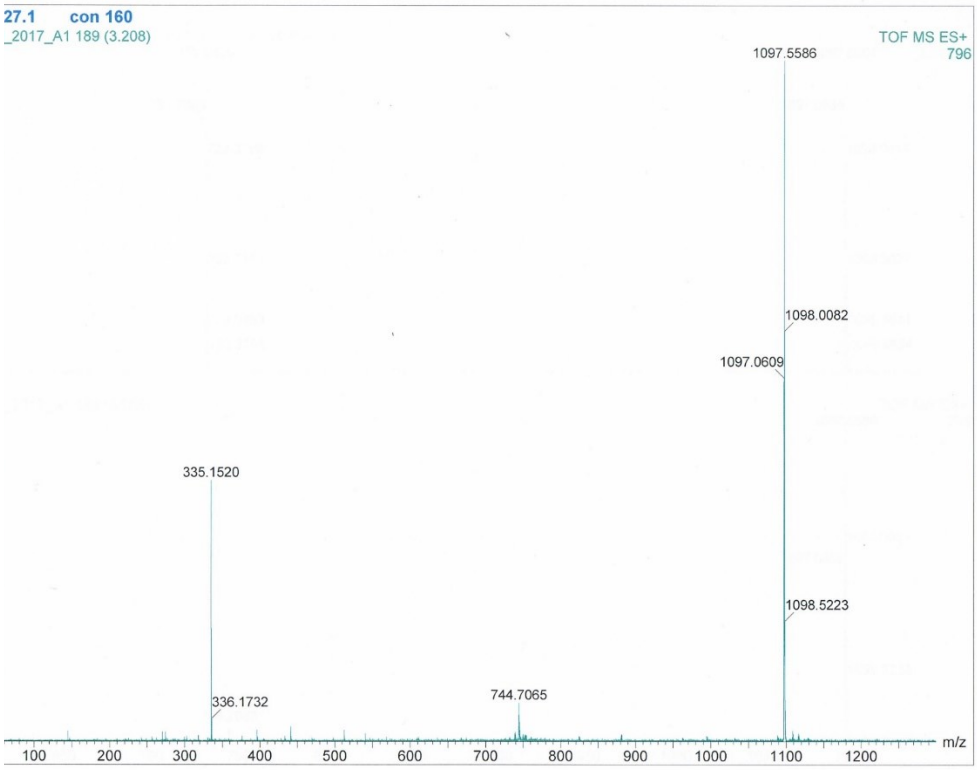
27.1 con 160
_2017_A1 189 (3.208)
TOF MS ES+
796
1097.5586
1098.0082
1097.0609
335.1520
1098.5223
336.1732
744.7065
m/z
100
200
300
400
500
600
700
800
900
1000
1100
1200

10

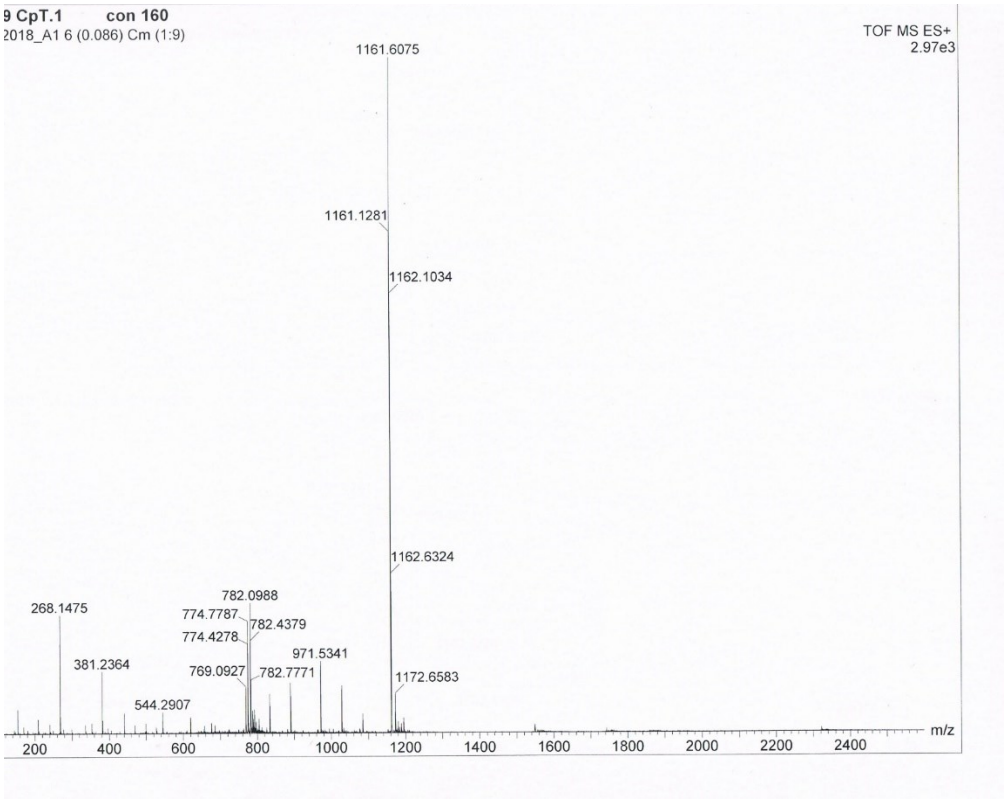
9 CpT.1 con 160
2018_A1 6 (0.086) Cm (1:9)
TOF MS ES+
2.97e3
1161.6075
1161.1281
1162.1034
1162.6324
782.0988
774.7787
782.4379
774.4278
971.5341
268.1475
381.2364
769.0927
782.7771
1172.6583
544.2907
m/z
200
400
600
800
1000
1200
1400
1600
1800
2000
2200
2400

11

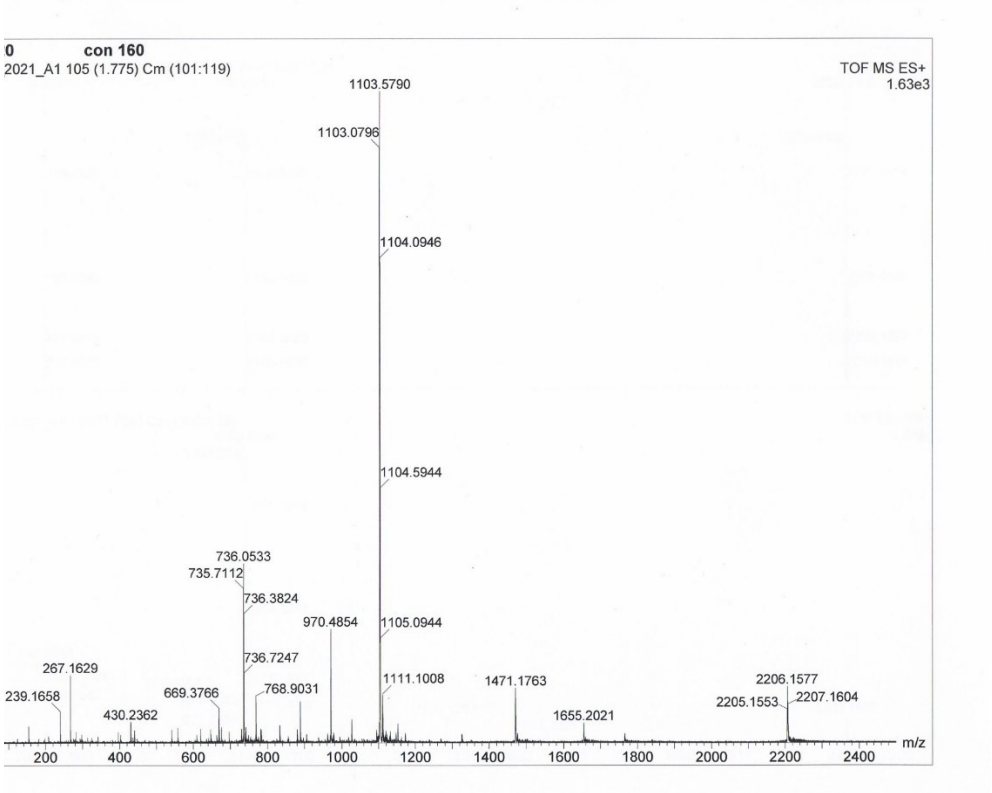
0 con 160
2021_A1 105 (1.775) Cm (101:119)
TOF MS ES+
1.63e3
1103.5790
1103.0796
1104.0946
1104.5944
736.0533
735.7112
736.3824
970.4854
1105.0944
736.7247
267.1629
1111.1008
1471.1763
2206.1577
239.1658
669.3766
768.9031
2205.1553
2207.1604
430.2362
1655.2021
m/z
200
400
600
800
1000
1200
1400
1600
1800
2000
2200
2400

12

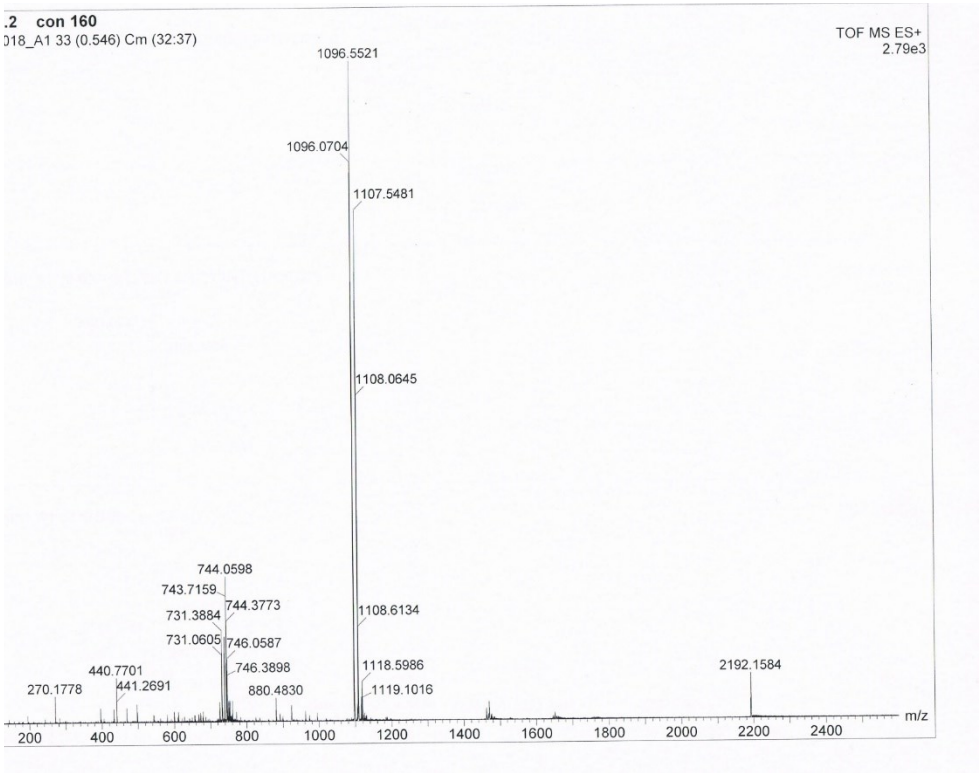
.2 con 160
018_A1 33 (0.546) Cm (32:37)
TOF MS ES+
2.79e3
1096.5521
1096.0704
1107.5481
1108.0645
744.0598
743.7159
744.3773
731.3884
731.0605
746.0587
746.3898
1108.6134
1118.5986
1119.1016
440.7701
441.2691
270.1778
880.4830
2192.1584
m/z
200
400
600
800
1000
1200
1400
1600
1800
2000
2200
2400

13

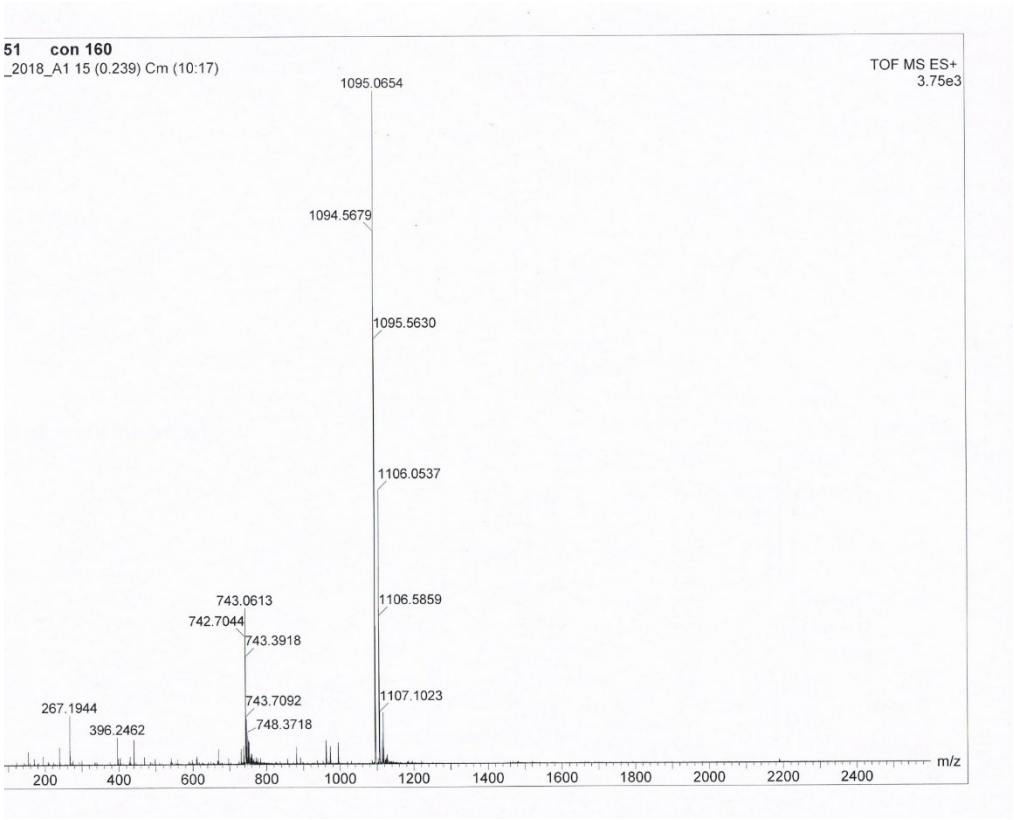
51 con 160
_2018_A1 15 (0.239) Cm (10:17)
TOF MS ES+
3.75e3
1095.0654
1094.5679
1095.5630
1106.0537
1106.5859
1107.1023
743.0613
742.7044
743.3918
743.7092
748.3718
267.1944
396.2462
m/z
200
400
600
800
1000
1200
1400
1600
1800
2000
2200
2400

14

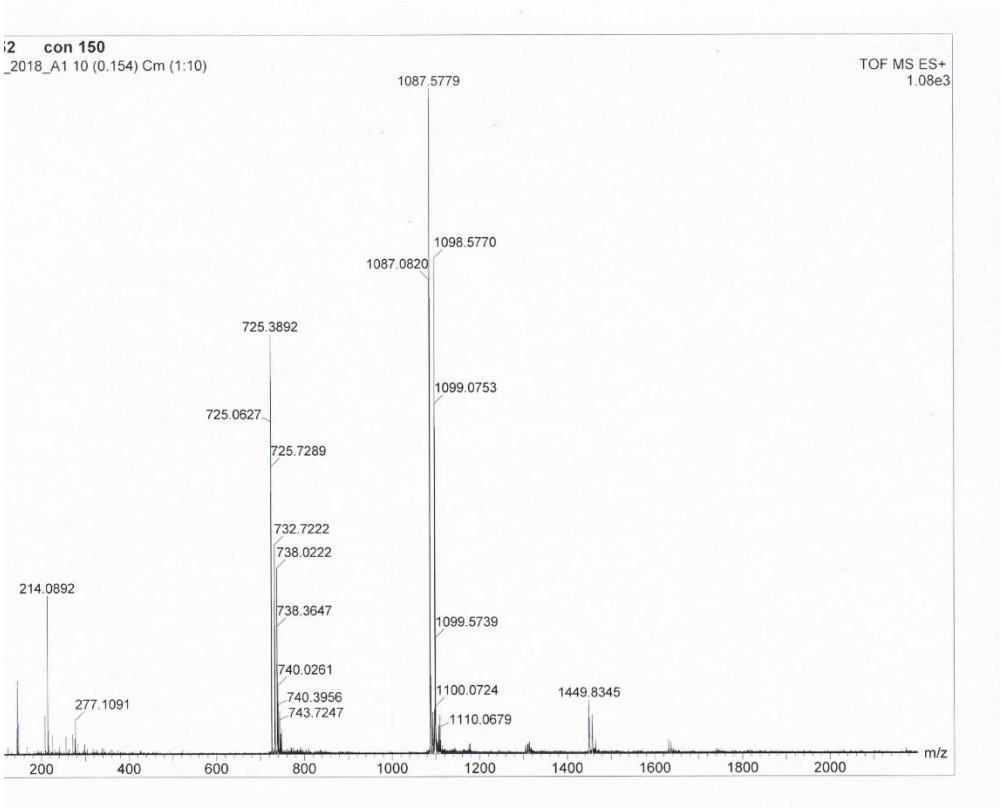
2 con 150
_2018_A1 10 (0.154) Cm (1:10)
TOF MS ES+
1.08e3
1087.5779
1098.5770
1087.0820
725.3892
1099.0753
725.0627
725.7289
732.7222
738.0222
214.0892
738.3647
1099.5739
740.0261
1100.0724
1449.8345
277.1091
740.3956
743.7247
1110.0679
m/z
200
400
600
800
1000
1200
1400
1600
1800
2000

15

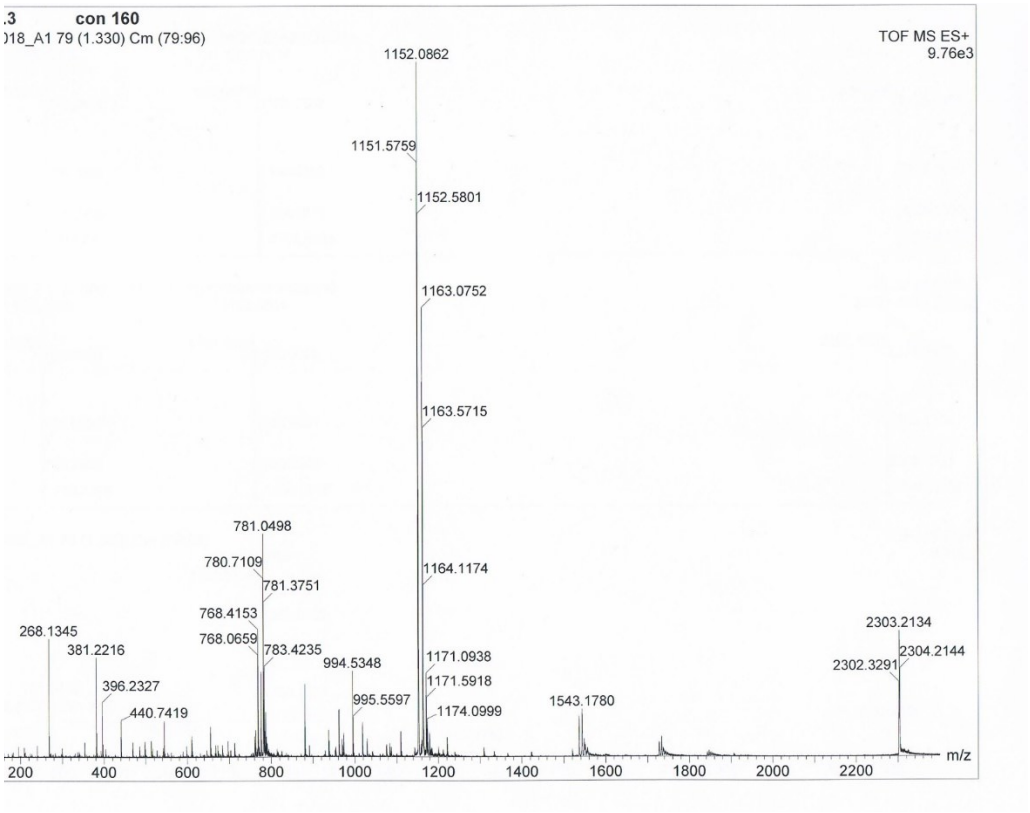
.3 con 160
)18_A1 79 (1.330) Cm (79:96)
TOF MS ES+
9.76e3
1152.0862
1151.5759
1152.5801
1163.0752
1163.5715
781.0498
780.7109
781.3751
1164.1174
768.4153
768.0659
783.4235
994.5348
1171.0938
1171.5918
995.5597
1174.0999
1543.1780
268.1345
381.2216
396.2327
440.7419
2303.2134
2304.2144
2302.3291
m/z
200
400
600
800
1000
1200
1400
1600
1800
2000
2200

16

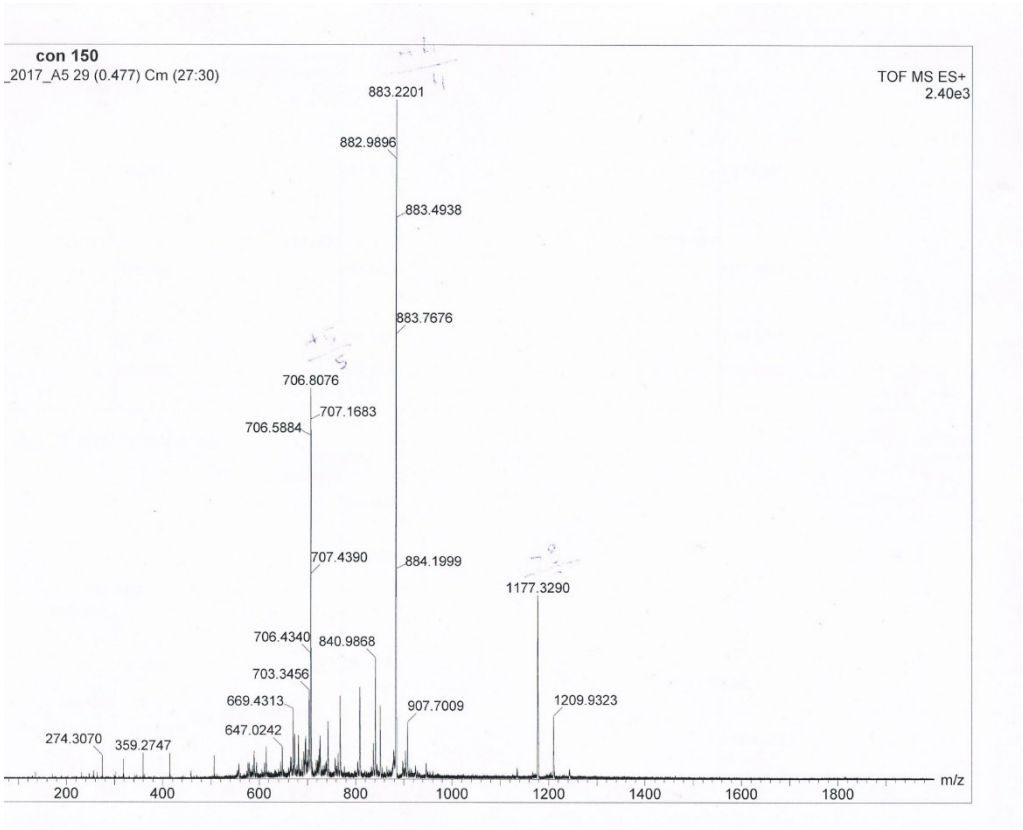
con 150
_2017_A5 29 (0.477) Cm (27:30)
TOF MS ES+
2.40e3
883.2201
882.9896
883.4938
883.7676
706.8076
707.1683
706.5884
707.4390
884.1999
1177.3290
706.4340
840.9868
703.3456
669.4313
907.7009
1209.9323
647.0242
274.3070
359.2747
m/z
200
400
600
800
1000
1200
1400
1600
1800

17

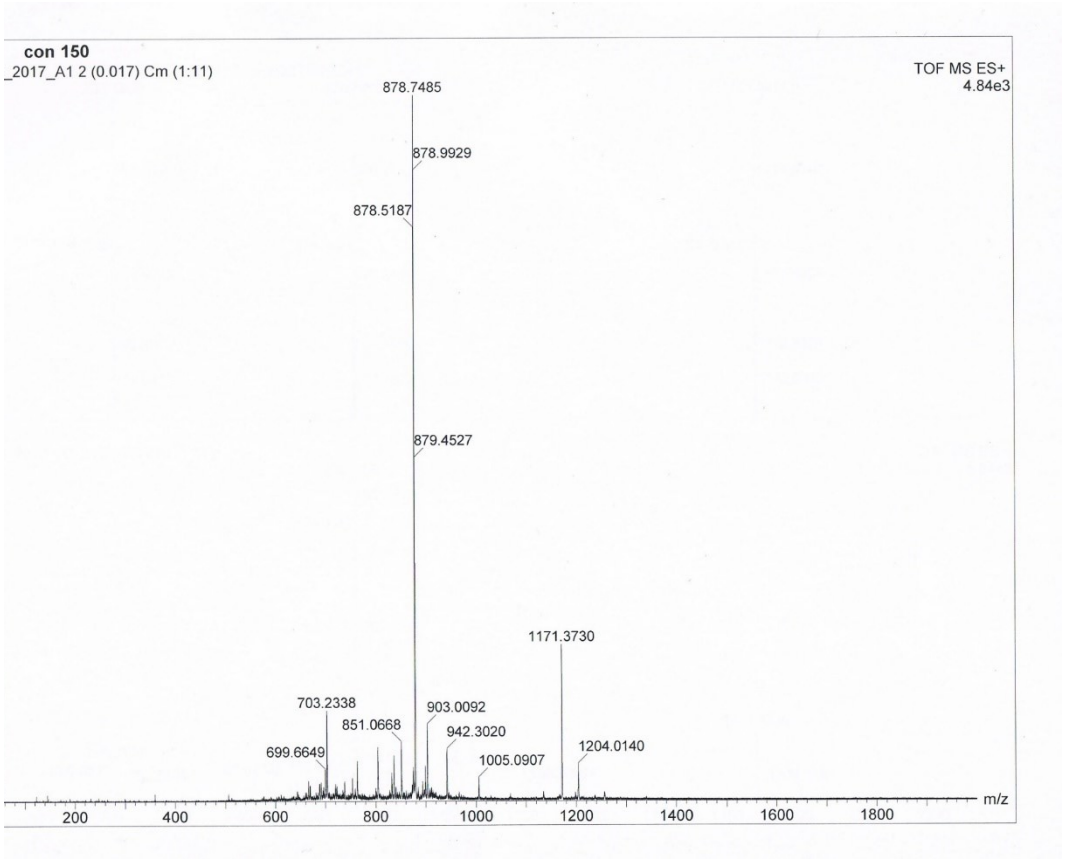
con 150
_2017_A1 2 (0.017) Cm (1:11)
TOF MS ES+
4.84e3
878.7485
878.9929
878.5187
879.4527
1171.3730
703.2338
903.0092
851.0668
942.3020
699.6649
1005.0907
1204.0140
m/z
200
400
600
800
1000
1200
1400
1600
1800

18

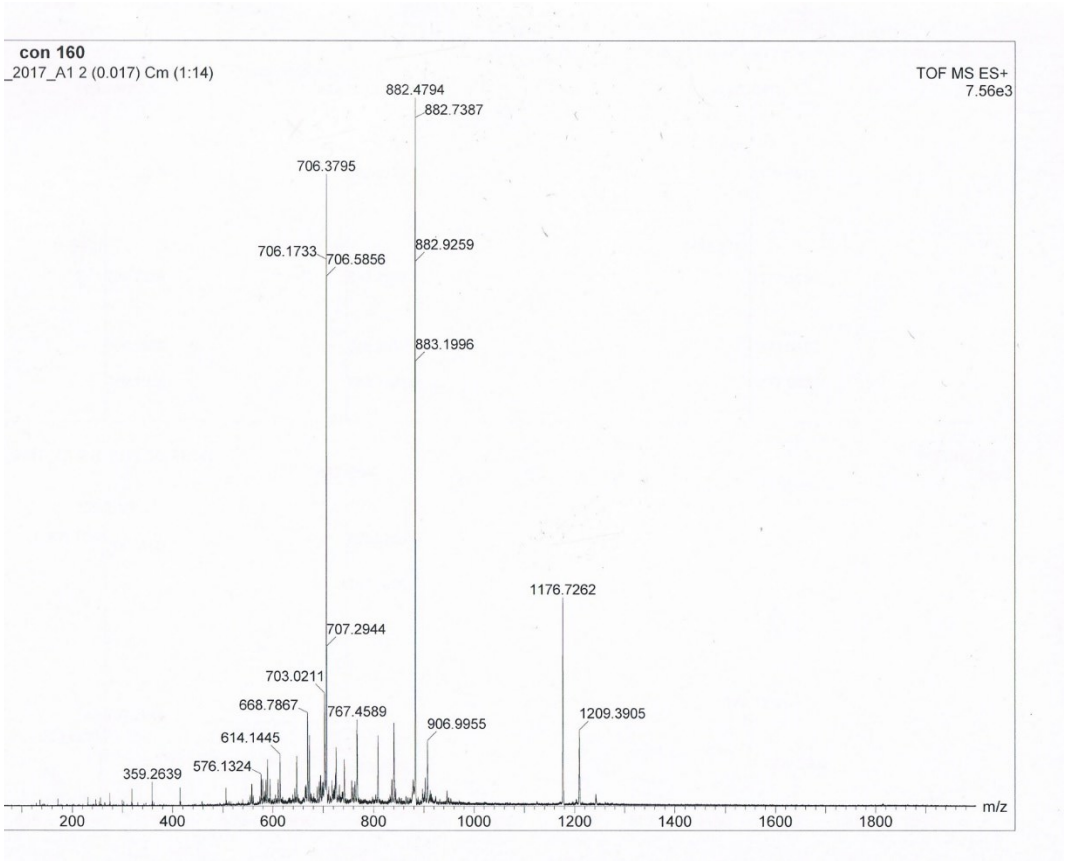
con 160
_2017_A1 2 (0.017) Cm (1:14)
TOF MS ES+
7.56e3
882.4794
882.7387
706.3795
706.1733
706.5856
882.9259
883.1996
1176.7262
707.2944
703.0211
668.7867
767.4589
906.9955
1209.3905
614.1445
576.1324
359.2639
200
400
600
800
1000
1200
1400
1600
1800
m/z

19

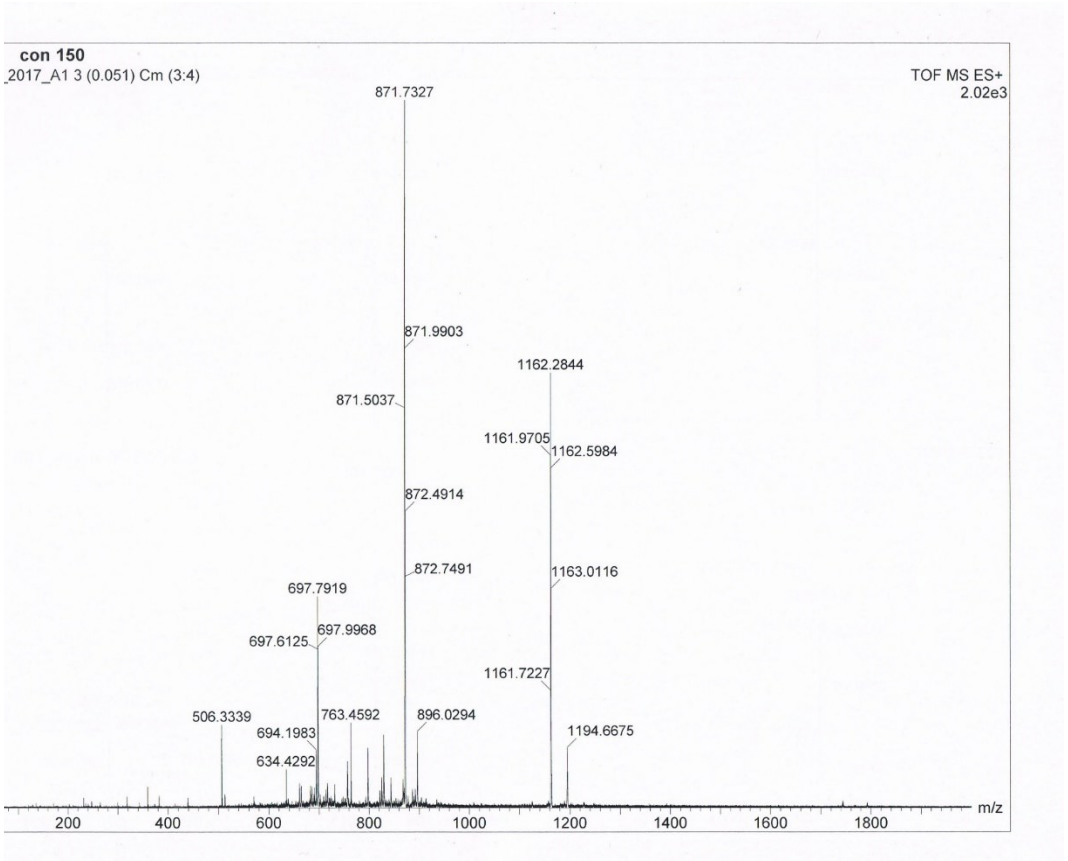
con 150
_2017_A1 3 (0.051) Cm (3:4)
TOF MS ES+
2.02e3
871.7327
871.9903
1162.2844
871.5037
1161.9705
1162.5984
872.4914
872.7491
1163.0116
697.7919
697.9968
697.6125
1161.7227
506.3339
763.4592
896.0294
694.1983
1194.6675
634.4292
m/z
200
400
600
800
1000
1200
1400
1600
1800

20

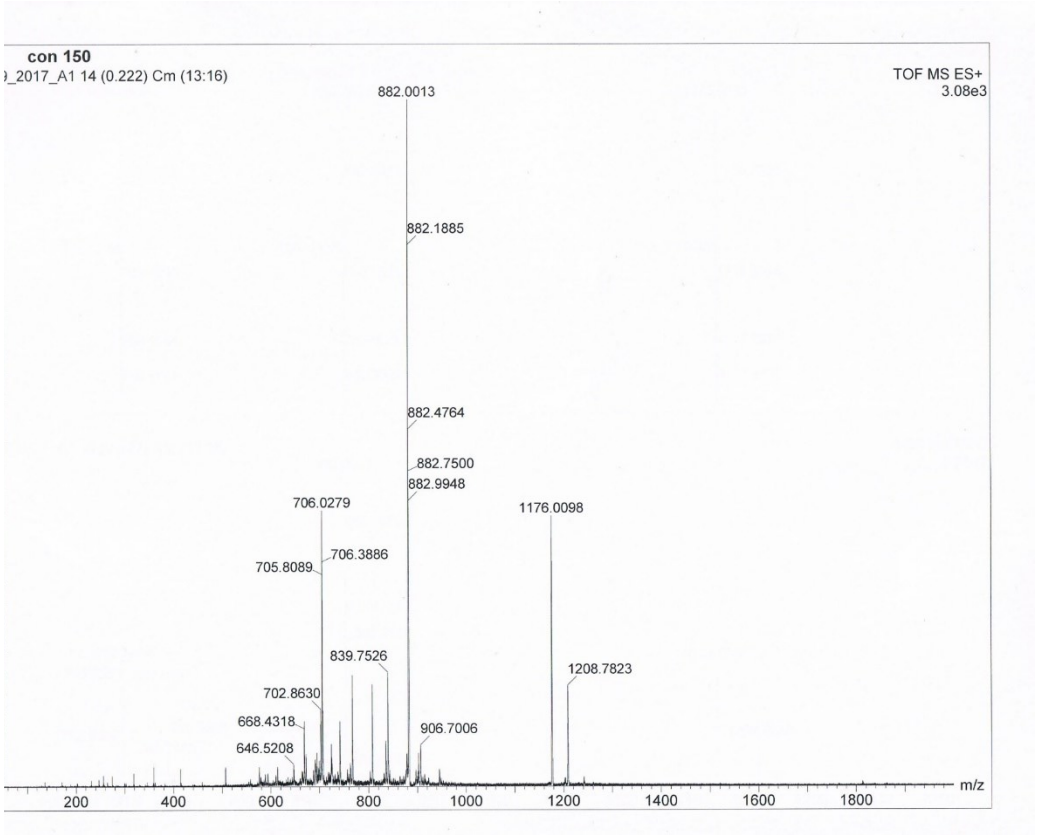
con 150
_2017_A1 14 (0.222) Cm (13:16)
TOF MS ES+
3.08e3
882.0013
882.1885
882.4764
882.7500
882.9948
706.0279
1176.0098
705.8089
706.3886
839.7526
1208.7823
702.8630
668.4318
906.7006
646.5208
m/z
200
400
600
800
1000
1200
1400
1600
1800

21

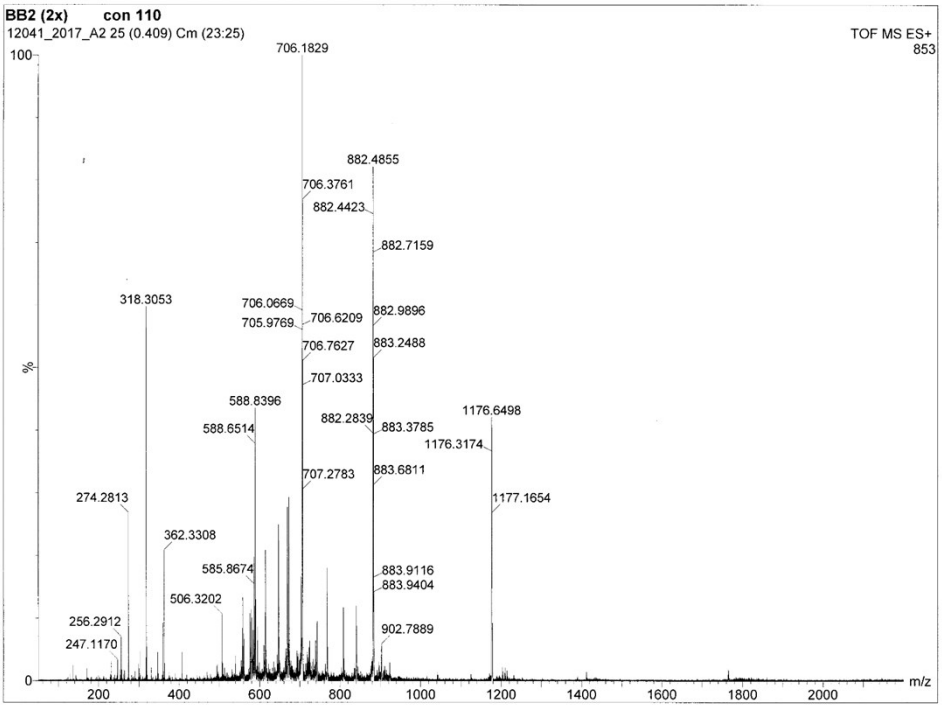
BB2 (2x) con 110
12041_2017_A2 25 (0.409) Cm (23:25)
TOF MS ES+
853
100
%
0
706.1829
882.4855
706.3761
882.4423
882.7159
318.3053
706.0669
705.9769
706.6209
882.9896
706.7627
883.2488
707.0333
588.8396
588.6514
882.2839
883.3785
1176.6498
1176.3174
707.2783
883.6811
274.2813
1177.1654
362.3308
585.8674
883.9116
883.9404
506.3202
256.2912
247.1170
902.7889
200
400
600
800
1000
1200
1400
1600
1800
2000
m/z

22

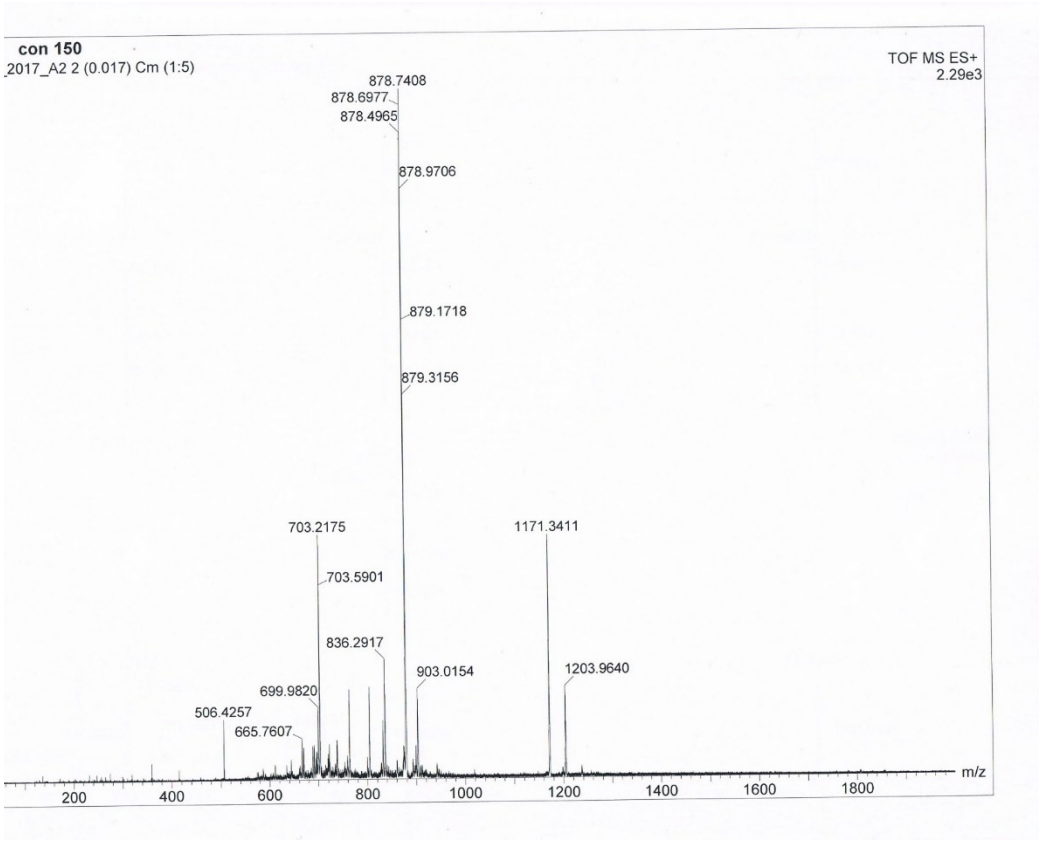
con 150
2017_A2 2 (0.017) Cm (1:5)
TOF MS ES+
2.29e3
878.7408
878.6977
878.4965
878.9706
879.1718
879.3156
703.2175
703.5901
836.2917
699.9820
506.4257
665.7607
903.0154
1171.3411
1203.9640
m/z
200
400
600
800
1000
1200
1400
1600
1800

23

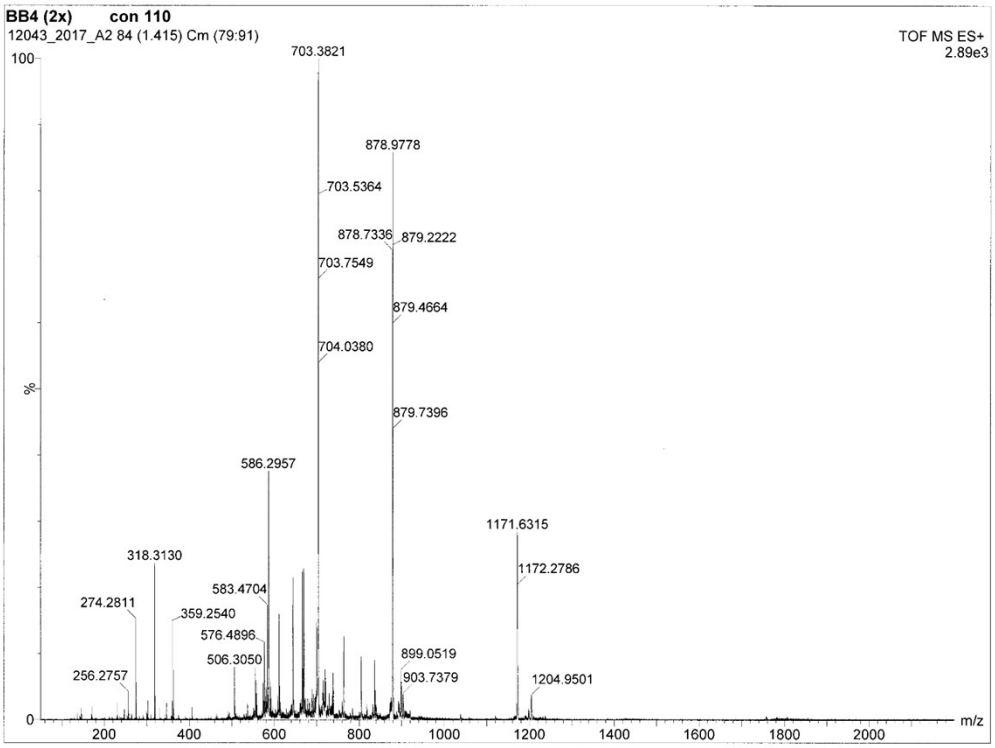
BB4 (2x) con 110
12043_2017_A2 84 (1.415) Cm (79:91)
TOF MS ES+
2.89e3
100
%
0
703.3821
878.9778
703.5364
878.7336
879.2222
703.7549
879.4664
704.0380
879.7396
586.2957
1171.6315
318.3130
1172.2786
583.4704
274.2811
359.2540
576.4896
506.3050
899.0519
256.2757
903.7379
1204.9501
200
400
600
800
1000
1200
1400
1600
1800
2000
m/z

24

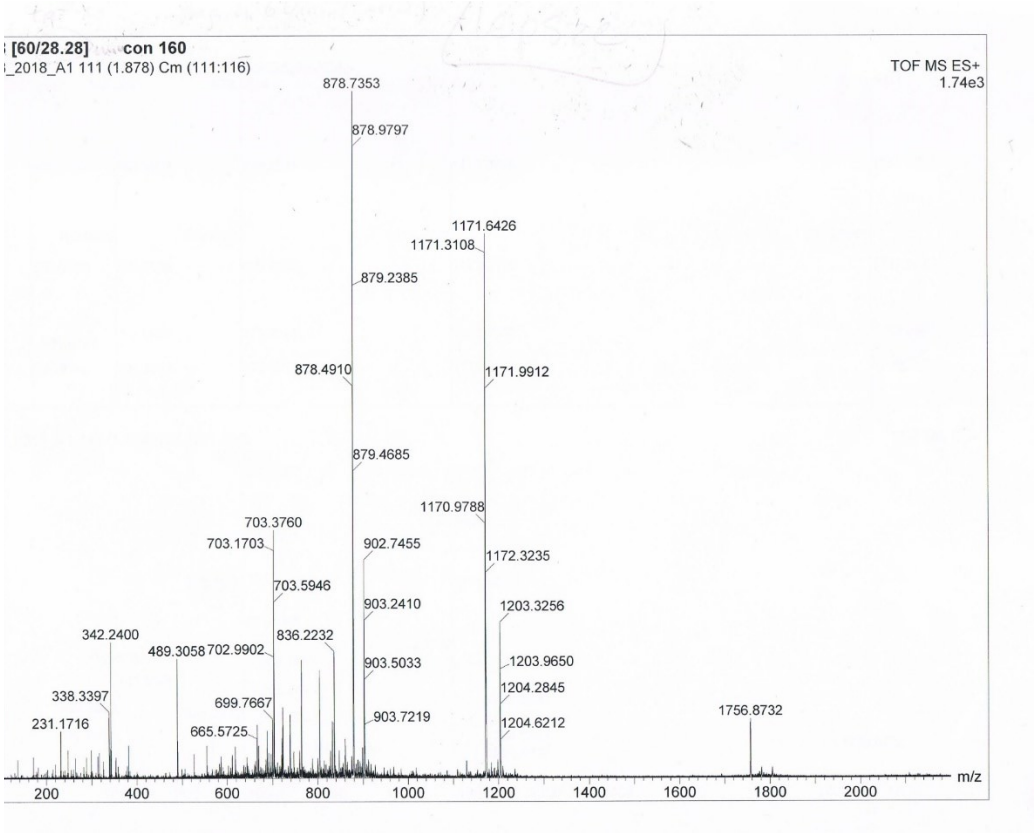
[60/28.28] con 160
_2018_A1 111 (1.878) Cm (111:116)
TOF MS ES+
1.74e3
878.7353
878.9797
1171.6426
1171.3108
879.2385
878.4910
1171.9912
879.4685
1170.9788
703.3760
703.1703
902.7455
1172.3235
703.5946
903.2410
1203.3256
342.2400
489.3058
702.9902
836.2232
903.5033
1203.9650
1204.2845
338.3397
699.7667
903.7219
1204.6212
1756.8732
231.1716
665.5725
m/z
200
400
600
800
1000
1200
1400
1600
1800
2000

25

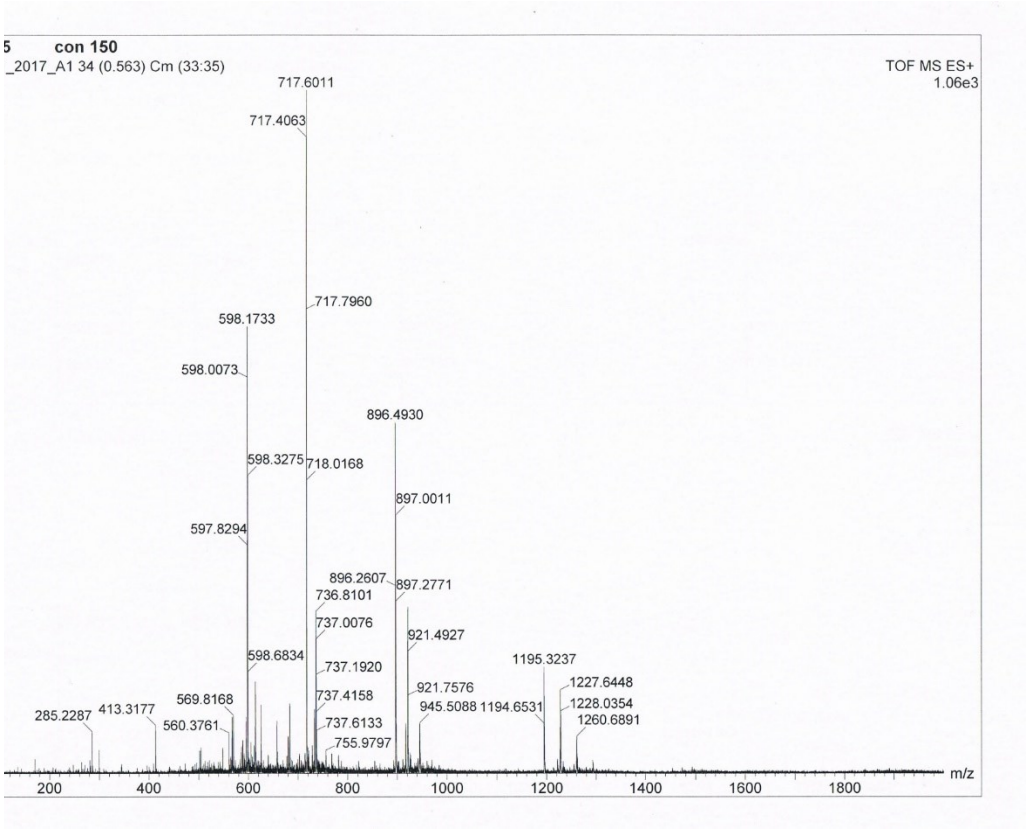
5 con 150
_2017_A1 34 (0.563) Cm (33:35)
TOF MS ES+
1.06e3
717.6011
717.4063
717.7960
598.1733
598.0073
896.4930
598.3275
718.0168
897.0011
597.8294
896.2607
897.2771
736.8101
737.0076
921.4927
598.6834
737.1920
1195.3237
1227.6448
921.7576
737.4158
569.8168
945.5088
1194.6531
1228.0354
285.2287
413.3177
560.3761
737.6133
1260.6891
755.9797
m/z
200
400
600
800
1000
1200
1400
1600
1800

26

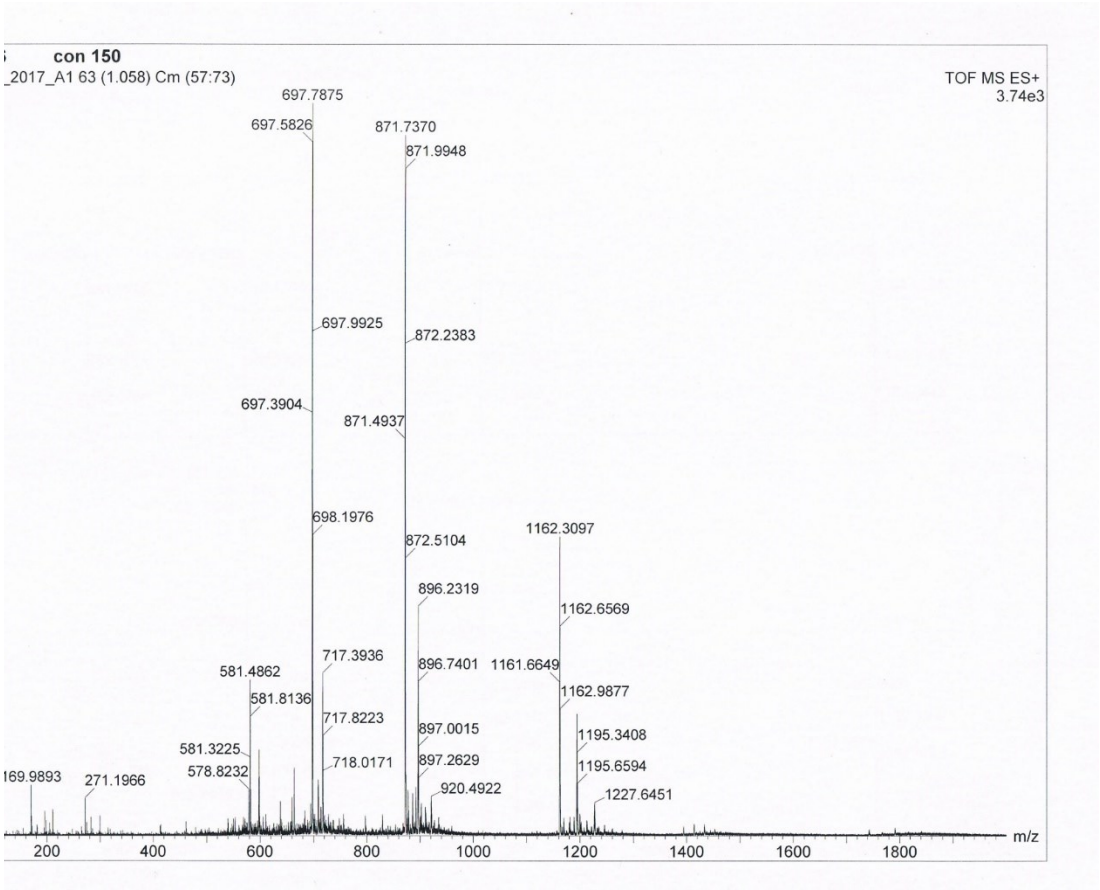
con 150
_2017_A1 63 (1.058) Cm (57:73)
TOF MS ES+
3.74e3
697.7875
697.5826
871.7370
871.9948
697.9925
872.2383
697.3904
871.4937
698.1976
872.5104
1162.3097
896.2319
1162.6569
717.3936
581.4862
896.7401
1161.6649
581.8136
1162.9877
717.8223
897.0015
1195.3408
581.3225
718.0171
897.2629
1195.6594
578.8232
920.4922
169.9893
271.1966
1227.6451
m/z
200
400
600
800
1000
1200
1400
1600
1800

27

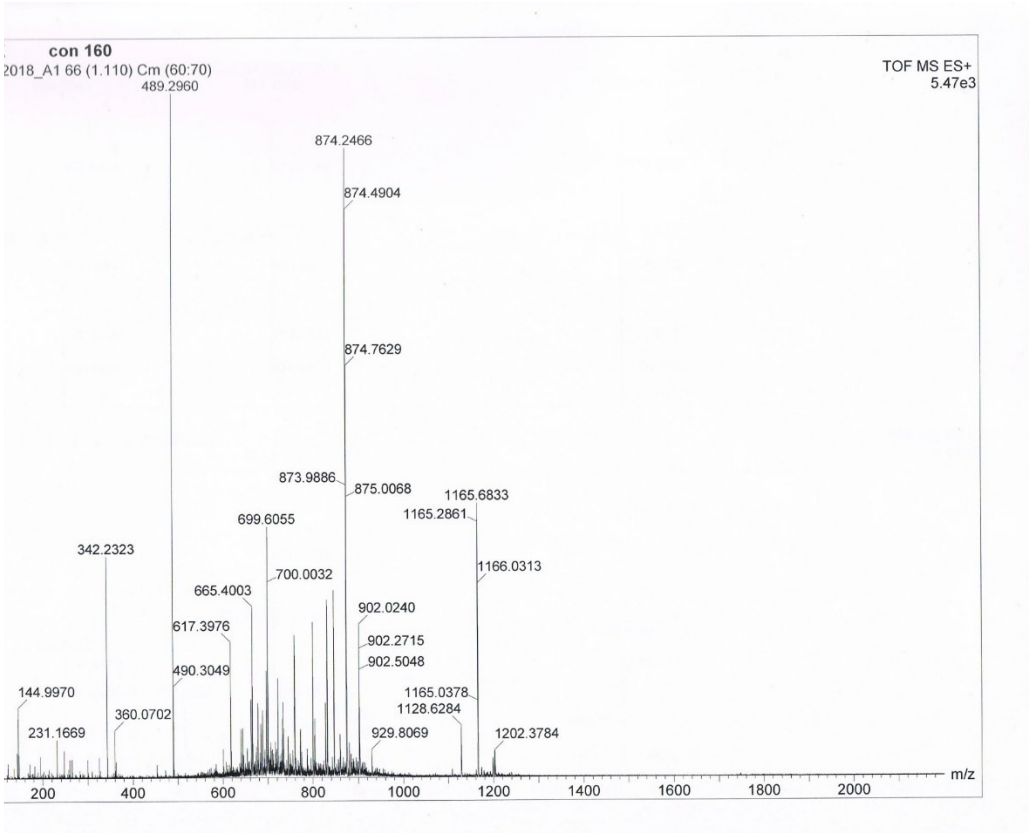
con 160
2018_A1 66 (1.110) Cm (60:70)
TOF MS ES+
5.47e3
489.2960
874.2466
874.4904
874.7629
873.9886
875.0068
1165.6833
1165.2861
699.6055
342.2323
1166.0313
700.0032
665.4003
902.0240
617.3976
902.2715
902.5048
490.3049
144.9970
1165.0378
1128.6284
360.0702
231.1669
929.8069
1202.3784
m/z
200
400
600
800
1000
1200
1400
1600
1800
2000

28

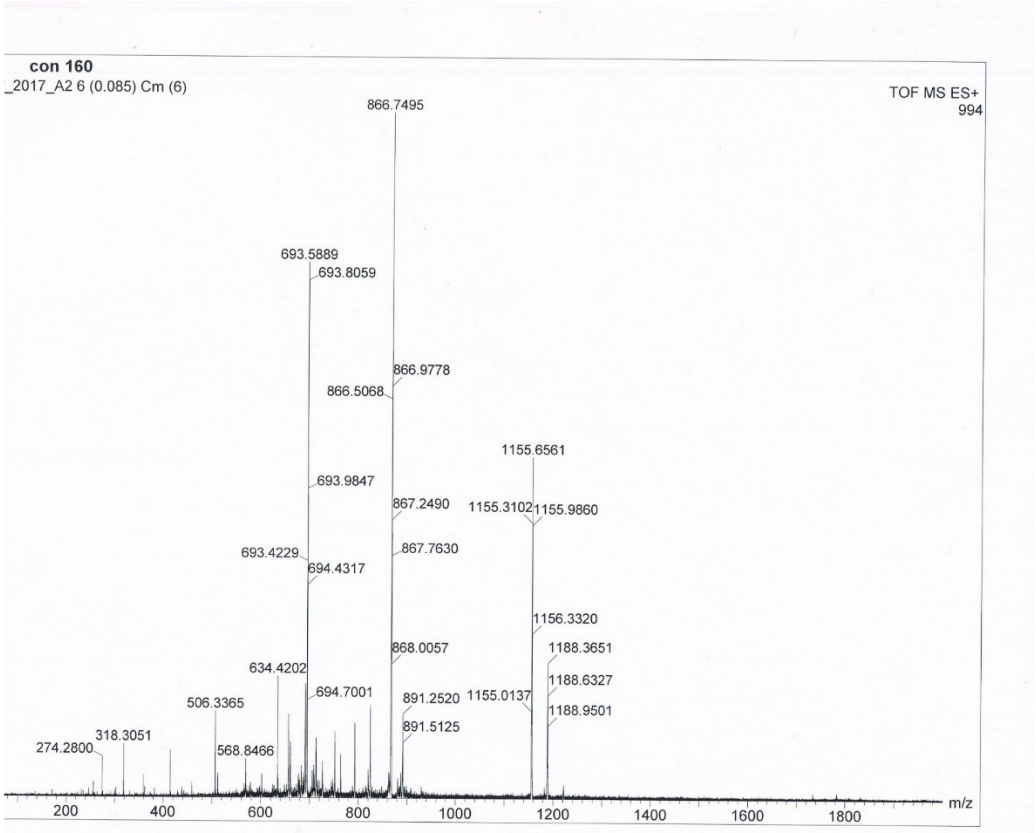
con 160
_2017_A2 6 (0.085) Cm (6)
TOF MS ES+
994
866.7495
693.5889
693.8059
866.9778
866.5068
1155.6561
693.9847
867.2490
1155.3102
1155.9860
693.4229
867.7630
694.4317
1156.3320
868.0057
1188.3651
634.4202
1188.6327
694.7001
891.2520
1155.0137
506.3365
1188.9501
891.5125
318.3051
274.2800
568.8466
200
400
600
800
1000
1200
1400
1600
1800
m/z

29

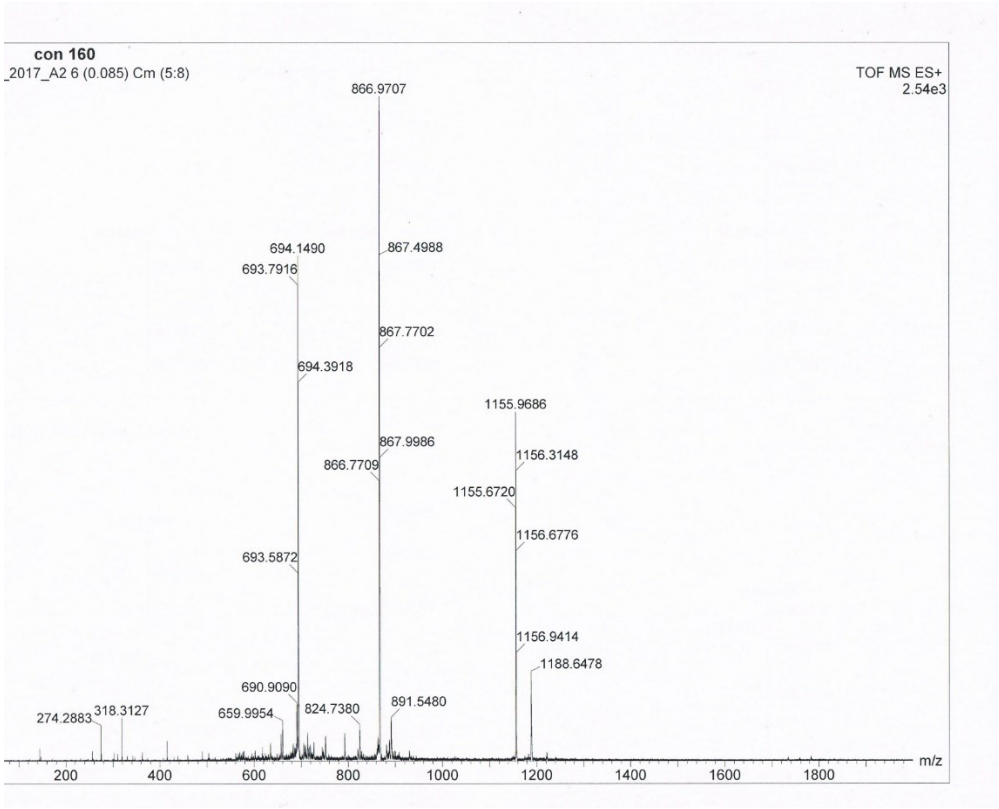
con 160
_2017_A2 6 (0.085) Cm (5:8)
TOF MS ES+
2.54e3
866.9707
694.1490
867.4988
693.7916
867.7702
694.3918
1155.9686
867.9986
1156.3148
866.7709
1155.6720
1156.6776
693.5872
1156.9414
1188.6478
690.9090
891.5480
274.2883
318.3127
659.9954
824.7380
m/z
200
400
600
800
1000
1200
1400
1600
1800